SAHC

Seismic Vulnerability Assessment of Masonry Churches Including Uncertainty

Cassandra Cullimore

Spain | 2018

ADVANCED MASTERS IN STRUCTURAL ANALYSIS
OF MONUMENTS AND HISTORICAL CONSTRUCTIONS

Master's Thesis

Cassandra Cullimore

Seismic Vulnerability Assessment of Masonry Churches Including Uncertainty

UNIVERSITAT POLITÈCNICA DE CATALUNYA

University of Minho

Education and Culture

Erasmus Mundus

ADVANCED MASTERS IN STRUCTURAL ANALYSIS
OF MONUMENTS AND HISTORICAL CONSTRUCTIONS

Master's Thesis

Cassandra Cullimore

Seismic Vulnerability Assessment of Masonry Churches Including Uncertainty

This Masters Course has been funded with support from the European Commission. This publication reflects the views only of the author, and the Commission cannot be held responsible for any use which may be made of the information contained therein.

Spain | 2018

DECLARATION

Name: Cassandra Cullimore

Email: cassie.cullimore@cmail.carleton.ca

Title of the Msc Dissertation: Seismic Vulnerability Assessment of Masonry Churches Including Uncertainty

Supervisor(s): Luca Pelà, Savvas Saloustros, José Matos

Year: 2018

I hereby declare that all information in this document has been obtained and presented in accordance with academic rules and ethical conduct. I also declare that, as required by these rules and conduct, I have fully cited and referenced all material and results that are not original to this work.

I hereby declare that the MSc Consortium responsible for the Advanced Masters in Structural Analysis of Monuments and Historical Constructions is allowed to store and make available electronically the present MSc Dissertation.

University: Technical University of Catalonia (UPC)

Date: July 23rd, 2018

Signature: 

This page is left blank on purpose.

To the many strong women in my life, who have shown me that work and dedication will always pay off.

This page is left blank on purpose.

ACKNOWLEDGEMENTS

I would like to thank my supervisors Luca Pelà and Savvas Saloustros, for their support, knowledge, and help in developing this research.

To all the SAHC professors, thank you for all the knowledge and guidance you have provided throughout this master's program.

Thank you to the SAHC Managing Board for awarding me with a SAHC Consortium Scholarship, making this degree financially feasible for me.

I would especially like to thank my family, for always supporting and encouraging me.

Finally, thank you to Jamie for your invaluable programming knowledge and for always believing in me.

This page is left blank on purpose.

ABSTRACT

All structures are susceptible to damage when experiencing seismic forces due to their destructive nature. However, masonry structures are particularly susceptible due to their low ductility and common lack of connection among the composing structural elements. As a result, there is a need for determining the seismic performance of masonry structures. However, there are numerous challenges in performing a seismic assessment on a masonry structure. These include the geometry, actions, assumptions made during the modelling process, and material properties. Specifically, with masonry there is an uncertainty in the material mechanical properties.

This work aims to investigate the effect of material mechanical property uncertainty on the seismic capacity of a case study, the Mallorca Cathedral on the Island of Mallorca, Spain. A two-dimensional finite element model of a typical bay was analyzed. This two-dimensional model was utilized to reduce the computational time required. The model was calibrated to a previous study through the comparison of results from a nonlinear static analysis of a detailed three-dimensional model. The seismic capacity was determined using nonlinear static analyses throughout the study of this structure. The uncertainty of the material properties was taken into account in the compressive strength, tensile strength, and Young's Modulus of the structural materials. These were defined as random variables and a Monte Carlo Simulation was used to obtain a population of 200 different models. These 200 models were analyzed using nonlinear static analyses to determine the seismic capacity. The capacity curves were then simplified into bilinear capacity curves and three damage grades were obtained as a function of the ultimate and yield displacement. Finally, fragility curves were derived for the Mallorca Cathedral. This was used to obtain the probability of each damage state relative to the peak ground acceleration of a real earthquake.

This page is left blank on purpose.

RESUMEN

Todas las estructuras son susceptibles al daño cuando experimentan fuerzas sísmicas debido a su naturaleza destructiva. Sin embargo, las estructuras de mampostería son particularmente susceptibles debido a su baja ductilidad y a la falta común de conexión entre los elementos estructurales que la componen. Como resultado, existe la necesidad de determinar las prestaciones sísmicas de las estructuras de mampostería. Sin embargo, existen numerosos desafíos al realizar una evaluación sísmica de una estructura de mampostería. Estos incluyen la geometría, las acciones, las hipótesis a considerar durante el proceso de modelado y las propiedades del material. Específicamente, con la mampostería existe una incertidumbre en las propiedades mecánicas del material.

Este trabajo tiene como objetivo investigar el efecto de la incertidumbre de las propiedades mecánicas en la capacidad sísmica de un caso de estudio, la Catedral de Mallorca, en la isla de Mallorca, España. Se analizó un modelo bidimensional de elementos finitos de una crujía típica. Este modelo bidimensional se utilizó para reducir el tiempo computacional requerido. El modelo fue calibrado mediante un estudio previo a través de la comparación de los resultados de un análisis estático no lineal de un modelo tridimensional detallado. La capacidad sísmica se determinó mediante análisis estáticos no lineales durante el estudio de esta estructura. La incertidumbre de las propiedades de los materiales se tuvo en cuenta en la resistencia a la compresión, la resistencia a la tracción y el módulo de Young de los materiales estructurales. Estos se definieron como variables aleatorias y se utilizó una simulación de Monte Carlo para obtener una población de 200 modelos diferentes. Estos 200 modelos se analizaron utilizando análisis estáticos no lineales para determinar la capacidad sísmica. Las curvas de capacidad se simplificaron luego en curvas de capacidad bilineal y se obtuvieron tres grados de daño en función del desplazamiento final y al límite elástico. Finalmente, se derivaron curvas de fragilidad para la Catedral de Mallorca, para obtener la probabilidad de cada grado de daño en relación con la aceleración máxima del terreno de un terremoto real.

This page is left blank on purpose.

TABLE OF CONTENTS

1. Introduction 1
1.1 Motivation 1
1.2 Objectives 2
1.3 Methodology 2
2. State of the Art 5
2.1 Vulnerability Assessment of Masonry Structures 5
2.2 Material Uncertainty of Masonry 6
2.3 Previous Similar Studies and Results 8
2.3.1 Seismic Assessment of Historical Masonry Construction Including Uncertainty 8
2.3.2 Vulnerability Assessment of Monumental Masonry Structures Including Uncertainty 10
2.3.3 Vulnerability Assessment of Masonry Churches Including Uncertainty 11
3. Case Study: Mallorca Cathedral 13
3.1 Introduction and History 13
3.2 Description 14
3.3 Previous Studies 16
4. Numerical Model 27
4.1 Finite Element Model 27
4.2 Equivalent Two-Dimensional Model 32
4.3 Nonlinear Static Analysis and Damage Pattern 33
5. Uncertainty Evaluation 39
5.1 Identified Random Variables 39
5.2 Monte Carlo Simulation 39
5.3 Reference Model 43
6. Probabilistic Seismic Assessment 47
6.1 Nonlinear Static Analyses – Capacity Curves 47
6.2 Application of the Mechanical Approach 52
6.2.1 Idealization of Capacity Curves 52
6.2.2 Definition of Damage Grades 54
6.2.3 Definition of Fragility Curves 55
6.3 Comparison to Similar Studies 56
7. Conclusions 59
7.1 Summary of Work 59
7.2 Conclusions of Research 59
7.3 Suggestions for Further Work 59
Bibliography 61

TABLE OF FIGURES

Figure 1 – Capacity Curves – Royal Monastery of Santa Maria de Poblet (Petromichelakis, Saloustros, & Pela, 2014) 9
Figure 2 – Fragility Curves of – Royal Monastery of Santa Maria de Poblet (Petromichelakis, Saloustros, & Pela, 2014) 9
Figure 3 - Capacity Curves – Santa Maria Del Mar Cathedral (Contrafatto, 2017) 10
Figure 4 – Fragility Curve of Santa Maria Del Mar (Contrafatto, 2017) 11
Figure 5 – Control Nodes Considered in the Application of the N2 Method – Santa Maria del Pi (Bitlloch, 2018) 12
Figure 6 – Fragility Curves of Node B of Santa Maria del Pi (Bitlloch, 2018) 12
Figure 7 - Map of Spain and Mallorca Island (Esri, 2018) 13
Figure 8 – Exterior View of Mallorca Cathedral (Trip Wolf, n.d.) 13
Figure 9 - Mallorca Cathedral - Sections (Roca, Cervera, Pela, Clemente, & Chiumenti, 2013) 15
Figure 10 - Mallorca Cathedral - Floor Plan (Roca, Cervera, Pela, Clemente, & Chiumenti, 2013) 15
Figure 11 – Thrust Line through Mallorca Cathedral (Rubió, 1912) 16
Figure 12 – Automatically Generated Thrust Lines (Maynou, 2001) 17
Figure 13 – Photo-Elastic Analysis (Mark, 1982) 17
Figure 14 – Deformed Shape and Stress Distribution at Collapse due to Wind Loading (Salas, 2002) 18
Figure 15 – Deformed Shape and Tensile Damage in Construction Analysis (a) First Stage Deformed Shape (b) First Stage Tensile Damage (c) Second Stage Deformed Shape (d) Second Stage Tensile Damage (Roca, Cervera, Pela, Clemente, & Chiumenti, 2013) 20
Figure 16 - Simulation of Long Term Deformation Including Effects of Construction Process - Deformed Shape (left) and Tensile Damage (right) (Roca, Cervera, Pela, Clemente, & Chiumenti, 2013) 21
Figure 17 - Finite Element Model of Study of the Effect of Ties Used During the Construction Process (a) Initial Construction with Ties (b) Complete Construction (c) Removal of Ties (Pela, Bourgeois, Roca, Cervera, & Chiumenti, 2016) 22
Figure 18 – Deformed Shape and Tensile Damage of Lateral Vault Without the Use of Ties During Construction (Left) and With Ties (Right) (Pela, Bourgeois, Roca, Cervera, & Chiumenti, 2016) 22
Figure 19 - Cracking Pattern and Sequence of Cracking at Collapse During Pushover Analysis in the Negative Y-Direction (Elyamani, 2015) 23
Figure 20 – Damage Pattern of Maximum Principal Strain with Deformed Shape at Maximum Negative Displacement During Nonlinear Dynamic Analysis in Longitudinal Direction (Elyamani, 2015) 24
Figure 21 - Damage Pattern of Maximum Principal Strain with Deformed Shape at Maximum Positive Displacement During Nonlinear Dynamic Analysis in Longitudinal Direction (Elyamani, 2015) 24
Figure 22 – Damage Pattern of Maximum Principal Strain with Deformed Shape During Nonlinear Dynamic Analysis in Transversal Direction (a) Maximum Negative Displacement (b) Maximum Positive Displacement (Elyamani, 2015) 25

Figure 23 – (a) Three-Dimensional Model Finite Element Model (Roca, Cervera, Pela, Clemente, & Chiumenti, 2013) (b) Two-Dimensional Model Finite Element Model 27
Figure 24 – Structural Elements of 2D Model 28
Figure 25 – Assumed Compression and Tension Behaviour 30
Figure 26 - Triangular Three Node Elements (DIANA FEA, 2017) 30
Figure 27 – Capacity Curve Comparison - Element Sizes Mesh 31
Figure 28 - Initial Finite Element Model Mesh 31
Figure 29 - Final Finite Element Model Mesh 31
Figure 30 - Comparison of Initial and Final Mesh Using Nonlinear Static Analysis 32
Figure 31 – Comparison of Capacity Curve of Equivalent Model to Reference Model (Roca, Cervera, Pela, Clemente, & Chiumenti, 2013) 33
Figure 32 - Capacity Curve - Equivalent Model 34
Figure 33 - First Developed Crack: Buttress Openings - 0.2 Self-Weight – Equivalent Model 35
Figure 34 – Crack Width in First Principle Direction Under Full Gravity Load – Equivalent Model 35
Figure 35 - Crack Width in First Principle Direction Under Maximum Loading Conditions of Pushover Analysis – Equivalent Model 36
Figure 36 - Crack Width in First Principle Direction Under Maximum Displacement of Pushover Analysis – Equivalent Model 37
Figure 37 – Deformed Shape and Tensile Damage (Roca, Cervera, Pela, Clemente, & Chiumenti, 2013) 37
Figure 38 - Frequency of Compressive Strength from Monte Carlo Simulation 42
Figure 39 - Frequency of Tensile Strength from Monte Carlo Simulation 43
Figure 40 - Frequency of Young's Modulus from Monte Carlo Simulation 43
Figure 41 – Comparison of Reference Model and Equivalent Model 44
Figure 42 – Contour of Crack Widths in the Principle Direction - First Developed Crack: Buttress Opening - 0.15 Self-Weight - Reference Model 45
Figure 43 – Contour of Crack Widths in First Principle Direction Under Gravity Load - Reference Model 45
Figure 44 – Contour Crack Widths in Frist Principle Direction at Maximum Load of Pushover Analysis - Reference Model 46
Figure 45 – 200 Capacity Curves from 200 Pushover Analyses Including 16^{th}, 50^{th}, and 84^{th} Percentile 47
Figure 46 – Reference, Mean, and Median Curve of Uncertainty Analysis 48
Figure 47 – Investigation in Post-Peak Behaviour – Decrease in Load Step Size, Continuing Convergence, Increase in Fracture Energy, and Change of Arc Length Control Point to Top of the Right Pier 49
Figure 48 - Collapse of Model A022: Model with Maximum Capacity 50
Figure 49 – Collapse of Model A029: Model with Median Capacity 51

Figure 50 – Collapse of Model A151: Model with Minimum Capacity 51
Figure 51 – Graphical Representation of N2 Method – Equivalent Single Degree of Freedom System (left) and Bilinear Capacity Curve (right) (IMIT, 2009)..... 52
Figure 52 – Bilinearization of Capacity Curve 54
Figure 53 – Damage Grades on Bilinear Idealized Capacity Curve..... 54
Figure 54 – Fragility Curve: Probability of Reaching Any Damage Grade for the Seismic Demand (PGA=0.04g) is Negligible 56
Figure 55 – Capacity Curves from Uncertainty Analysis – Royal Monastery of Santa Maria de Poblet (Petromichelakis, Saloustros, & Pela, 2014) 57
Figure 56 - Capacity Curves from Uncertainty Analysis – Santa Maria Del Mar Cathedral (Contrafatto, 2017)..... 57
Figure 57 – Capacity Curves from Uncertainty Analysis – Santa Maria Del Pi (Bitlloch, 2018)..... 58

TABLE OF TABLES

Table 1 – Variation of the Compressive Strength, Shear Strength, Young's Modulus for Different Masonry Typologies According to Table C8A.2.1 (CNR-DT, 2013) 6
Table 2 – Comparison of Mechanical Properties of a Masonry Wall Obtained in Experimental Results and Italian Code (Magenes, Penna, Galasco, & Rota, 2010) 8
Table 3 - Mechanical Properties from (Roca, Cervera, Pela, Clemente, & Chiumenti, 2013) 29
Table 4 - Thicknesses Used in Two-Dimensional Model (Roca, Cervera, Pela, Clemente, & Chiumenti, 2013) 29
Table 5 – Variables Used in Monte Carlo Simulation 40
Table 6 - Compressive Strength Minimum and Maximum Values Used in Monte Carlo Simulation (IMIT, 2009) 40
Table 7 – Minimum, Maximum, and Mean Material Properties Used in Monte Carlo Simulation (IMIT, 2009) 41
Table 8 – Dependent Materials' Percentage Coefficients 41
Table 9 - Logarithmic Mean and Deviation of Random Variables for Reference Material 42
Table 10 - Material Properties of Reference Model 43
Table 11 – Mechanical Properties of Representative Models of Uncertainty Analysis 49
Table 12 - Damage Grades (Lagomarsino & Giovinazzi, 2006) 54
Table 13 – Values for Elastic Response Spectra from Eurocode 6 55

1. INTRODUCTION

The following section provides a short introduction into the motivation behind this research, the objective milestones, and the methodology used throughout the presented dissertation on the Seismic Vulnerability Assessment of Masonry Churches Including Uncertainty.

1.1 Motivation

There are approximately 12,000-14,000 earthquakes detected each year, but many of these earthquakes are not severe enough to be felt by humans. Buildings start to exhibit damage when earthquakes have a magnitude of five or higher on the Richter Magnitude Scale, this accounts for approximately 1,640 of the detected earthquakes per year (Incorporated Research Institutions for Seismology, 2011). All structures are susceptible to damage due to the destructive nature of seismic forces, however, masonry structures are the most susceptible (D'Ayala, 2015). The earthquake of 2012 in Emilia-Romagna, Italy is a prime example of how masonry structures are affected and have an increased susceptibility to damage, as the majority of the damaged and collapsed structures were churches (Petromichelakis, Saloustros, & Pela, 2014). Masonry structures are particularly susceptible to damage during a seismic event due to the low ductility of the material and a common lack of connection between the elements. Because of this susceptibility, vulnerability assessments and structural analyses of existing masonry structures are necessary to determine if interventions or strengthening measures need to be taken to ensure a structure's stability during a seismic event.

There are several challenges when performing a structural analysis, especially on historic masonry structures, including the geometry, actions, and material. The geometry of the structure can be very complex, combining many types of members. The internal morphology and connections are often non-homogenous and are difficult to characterize even when using non-destructive or minor-destructive testing. There are also multiple different types of actions that the structure experiences throughout it's lifetime that may need to be considered in the analysis such as seismic, environmental, anthropogenic, cyclic, and gradual loads. Some of the alterations and damage experienced may also affect the analysis. In terms of material, masonry has a complex mechanical response. It presents brittle response in tension, frictional in shear, and its very sensitive to the orientation of the applied load (Roca, Cervera, Garlup, & Pela, 2010). All these factors increase the uncertainty and complexity of a vulnerability assessment of masonry structures. Material property uncertainty increases the uncertainty of the potential seismic capacity when performing a seismic assessment. As seen in previous studies a variation in the material properties can result in obtaining multiple collapse mechanisms (Contrafatto, 2017).

There are few case studies on the seismic vulnerability of masonry churches. Some of the case studies include (Petromichelakis, Saloustros, & Pela, 2014) and (Contrafatto, 2017), which will be discussed further in sections 2.3.1 and 2.3.2, respectively.

The uncertainty of the mechanical material properties in the vulnerability assessment of a masonry structure was the key motivation for this research. Numerous studies have been completed on the case study considered for this analysis, the Mallorca Cathedral, which will be discussed in Section 3.3, but all of these studies considered only deterministic values for the material properties. Therefore, it was concluded that the Mallorca Cathedral would be an appropriate case study to apply probabilistic material property values.

1.2 Objectives

The overall objective of this dissertation is to apply a seismic vulnerability assessment of a macro-element of the Mallorca Cathedral. More precisely, the proposed method applied to other church typologies completed by (Contrafatto, 2017), and (Petromichelakis, Saloustros, & Pela, 2014). This is obtained with completing the following more specific objectives.

Preparation of a two-dimensional model equivalent to (Roca, Cervera, Pela, Clemente, & Chiumenti, 2013) of the Mallorca Cathedral.

Assessment of the seismic response through pushover analysis.

Assessment of the possible variation of material properties and the effect on the seismic response of the structure. Preparation of numerous instances of the structure through Monte Carlo Simulation.

The variability of the response to an earthquake will be determined with the use of capacity and fragility curves. Capacity curves present the structural response to horizontal seismic actions, while fragility curves derive the probability of damage equal to or higher than a specific state for different levels of seismic intensity (Lagomarsino & Giovinazzi, 2006). From these obtained results a comparison to previous studies conducted by (Petromichelakis, Saloustros, & Pela, 2014) and (Contrafatto, 2017) is to be completed.

1.3 Methodology

The methodology used over the course of this research was based on the methodology used in (Contrafatto, 2017). To begin a model of a typical bay of the case study, the Mallorca Cathedral in Spain was developed. This was done by constructing an equivalent two-dimensional plane stress finite element model. This model was compared to past research completed by (Roca, Cervera, Pela, Clemente, & Chiumenti, 2013) to derive the numerical model to experience the same behaviour as a three-dimensional model. The seismic performance of this model was determined using structural nonlinear analyses by applying pushover analyses to the model. This type of analysis was used to determine the effect of the uncertainty of the mechanical properties on the structural response. The uncertainty of the mechanical properties was simulated by defining three random variables for each of the different materials found within the structure. These variables were the tensile strength, compressive strength, and elastic modulus of the structure. The values of the random variables were then determined

using a Monte Carlo simulation which generated a population of 200 possible parameters. A Monte Carlo Simulation is a mathematical process used to generate a set of numbers. These generated values were within the Italian Code guidelines for masonry material properties to ensure realistic mechanical properties. The mechanical approach is a capacity spectrum-based method, which the capacity is determined based on the intersection of the capacity curve and the earthquake demand. The N2 method was applied to determine the earthquake demand for a performance point. First, idealized capacity curves, elasto-plastic bilinear curves, were created. Using the capacity curve obtained from pushover analysis to obtain an equivalent single degree of freedom capacity curve. Damage grades were defined using the formulations suggested by (Lagomarsino & Giovinazzi, 2006), as a function of the yield displacement and ultimate displacement of the bilinear capacity curve. Lastly, fragility curves were derived to determine the probability of damage equal to each limit state. Using the generated results, a comparison to previous similar studies was conducted.

2. STATE OF THE ART

Some of the studies on vulnerability assessments of masonry structures and the uncertainty of masonry are discussed in follow sections. As well as similar studies to the research presented in this dissertation.

2.1 Vulnerability Assessment of Masonry Structures

There are numerous methods that can be used to perform vulnerability assessments on masonry structures. Three approaches will be discussed; empirical, analytical, and hybrid approaches.

Empirical methods are vulnerability assessments based on recorded damage from past earthquakes (Eleftheriado & Karabinis, 2013). There are multiple empirical methods that can be used in a vulnerability assessment, including damage probability matrix (DPM) and vulnerability index method (VIM). DPM is a method based on observation. This method relies on a lot of observed damage data from past earthquakes and correlates this data to the construction materials. Therefore, this method is highly dependent on the amount of seismic and architectural information available, which can be limited (D'Ayala, 2015). DPM describes the probability of a damage level occurring if a seismic event of a specified intensity level were to occur (Eleftheriado & Karabinis, 2013). While, VIM is a sum of weighted parameters associated with the structural and non-structural features of the building. These features are then given a class based on the behaviour during an earthquake. Class A induces good behaviour, Class C induces bad behaviour, and Class B induces an intermediate behaviour. Each class relates to a weighting factor k_i which is used to calculate the vulnerability index in equation (1) (Amellal, Bensaibi, & Grine, 2012).

$$VI = \sum_{i=1}^{N} k_i \tag{1}$$

The use of vulnerability index method can be used to correlate previous seismic damage with measurements of seismic actions allows for the comparison between different seismic zones (D'Ayala, 2015).

Another approach is the use of analytical methods. Analytical methods define a relationship between the structural response to seismic action and the damage. The reliability of this type of seismic vulnerability assessment depends on the modelling capabilities and the assumptions made during the modelling process (Eleftheriado & Karabinis, 2013). Some of the analytical methods include mechanism method, and capacity spectrum-based method. Mechanism method estimates the vulnerability indices through the application of kinematic models. Kinematic models determine collapse load factor multipliers of a combination of macro-elements and loads by imposing kinetic energy equations. Capacity spectrum-based method estimates seismic performance through the comparison of seismic capacity and seismic demand. This is completed using acceleration displacement response spectrum that is reduced to consider inelastic behaviour (Novelli, 2017).

Empirical methods are suitable for large scale studies while analytical methods are more appropriate for the study of specific buildings. To use the benefits of both empirical and analytical methods hybrid methods were developed. Hybrid methods combine statistics from earthquake damage with behaviour developed through pushover analyses. This is useful when damage data is only partially available. However, this may not diminish the uncertainty of the output because direct cross-correlation is not obtainable for different data sources resulting from different procedures (D'Ayala, 2015).

2.2 Material Uncertainty of Masonry

Masonry is a heterogeneous material comprised of mortar and some type of block typically brick or stone. Therefore, this makes it more difficult to understand the mechanical properties when compared to a material like steel or lumber that is homogenous. Less studies have been completed on masonry to determine the mechanical behaviour compared to other heterogenous materials like concrete and homogenous materials such as steel.

The variation of material properties of masonry is demonstrated in table C8A.2.1 from the Italian Code, this table can be seen below in Table 1. This table is used to approximate the mechanical properties of masonry based on different masonry typologies found in Italy, classified by visual inspection.

Table 1 – Variation of the Compressive Strength, Shear Strength, Young's Modulus for Different Masonry Typologies According to Table C8A.2.1 (CNR-DT, 2013)

Masonry Typology	f_c [N/mm^2]	τ_0 [N/mm^2]	E [N/mm^2]	G [N/mm^2]
	Min-Max	Min-Max	Min-Max	Min-Max
1 – Irregular stone Masonry	1	0.02	690	230
	1.8	0.032	1050	350
2 – Uncut Stone with Facing Walls of Limited Thickness and Infill Core	2	0.035	1020	340
	3	0.051	1440	480
3 – Cut Stone with Good Bond	2.6	0.056	1500	500
	3.8	0.074	1980	660
4 - Soft Stone with Good Bond	1.4	0.028	900	300
	2.4	0.042	1260	420
5 – Dressed Rectangular Stone Masonry	6	0.09	2400	780
	8	0.12	3200	940
6 - Full Brick Masonry with Lime Mortar	2.4	0.06	1200	400

	4	0.092	1800	600
7 – Masonry in Half-Filled Brick Blocks with Cement Mortar	5	0.24	3500	875
	8	0.32	5600	1400
8 – Hollow Brick Masonry	4	0.3	3600	1080
	6	0.4	5400	1620
9 – Hollow Brick Masonry with Dry Prepend Joints	3	0.1	2700	810
	4	0.13	3600	1080
10 – Concrete Block Masonry	1.5	0.095	1200	300
	2	0.125	1600	400
11 – Masonry in Half-Filled Concrete Blocks	3	0.18	2400	600
	4.4	0.24	3520	880

The above ranges show the uncertainty of the mechanical properties, even if the typology of the masonry is known. For example, the compressive strength of category seven masonry in half-filled brick blocks with cement mortar ranges from 5N/mm^2 to 8N/mm^2.

In comparison, a study performed by Magenes et al. (Magenes, Penna, Galasco, & Rota, 2010) with experimental tests to define mechanical properties through vertical compression, diagonal compression, and in-plane cyclic shear tests is presented in the following. In this study, a double lead wall with through stones constructed with irregular stones was considered. There were no specific standards for stone walls so the requirements for new masonry typologies were applied. During the vertical compression test, deformation was measured to determine the Young's modulus and Poisson's ratio of the wall. A diagonal compression test was used to determine the mechanical properties during the application of shear forces including the shear stiffness and strength. During this study specifically, the ultimate tensile strength and shear modulus were derived. From this study scattered results were obtained when determining the mechanical properties of the masonry wall. The largest variation was observed in the tensile strength obtained from the diagonal compression test, with a coefficient of variation of 21.8%. While the compressive strength variation was the least, with a coefficient of variation of 8%. The Young's modulus and shear modulus also had varying results with a coefficient of variation of 13.5% and 14.8% respectfully. These results were then compared to the Italian Code recommendations from Table C8A.2.1 the material category considered was "undressed stone masonry with regular texture". This comparison is shown in Table 2.

Table 2 – Comparison of Mechanical Properties of a Masonry Wall Obtained in Experimental Results and Italian Code (Magenes, Penna, Galasco, & Rota, 2010)

Mechanical Properties	Experiments		Code	
	Variation	Mean	Variation	Mean
f_m [MPa]	3.07-3.48	3.28	2.60-3.80	3.20
f_t [MPa]	0.112-0.161	0.14	0.084-0.111	0.10
E [MPa]	22.73-28.26	25.50	15.0-19.8	17.40
G [MPa]	7.39-9.40	8.40	5.0-6.6	5.80

There was a good correspondence when comparing the results especially with the compressive strength, but there were many instances where there were differences between the experimental results and the code. The experimental Young's modulus was notably higher than the code, as well as the shear modulus. This study shows that even though tests were performed, there was a lot of variability in the mechanical properties (Magenes, Penna, Galasco, & Rota, 2010).

2.3 Previous Similar Studies and Results

2.3.1 Seismic Assessment of Historical Masonry Construction Including Uncertainty

In a study conducted by (Petromichelakis, Saloustros, & Pela, 2014) the Royal Monastery of Santa Maria de Poblet in Spain was considered for a seismic vulnerability assessment. An equivalent two-dimensional finite element model of a typical bay was developed to determine the capacity of the structure. In this study, the effect of uncertainty in the material properties was considered using a Monte Carlo Simulation to generate a population of possible material properties. Deterministic values obtained from previous in-situ testing and suggestions from (P.I.E.T 70, 1971) and (Italian Ministry of Infrastructure and Transport, 2009). From the deterministic values the variation was determined from values obtained from (P.I.E.T 70, 1971) and (Italian Ministry of Infrastructure and Transport, 2009). Six parameters were considered for the Monte Carlo Simulation compressive strength, tensile strength, Young's modulus, density, tensile fracture energy, and infill of lateral vaults. Using these properties pushover analyses were performed. This showed how the variation of the properties affected the capacity of the structure, as seen in Figure 1.

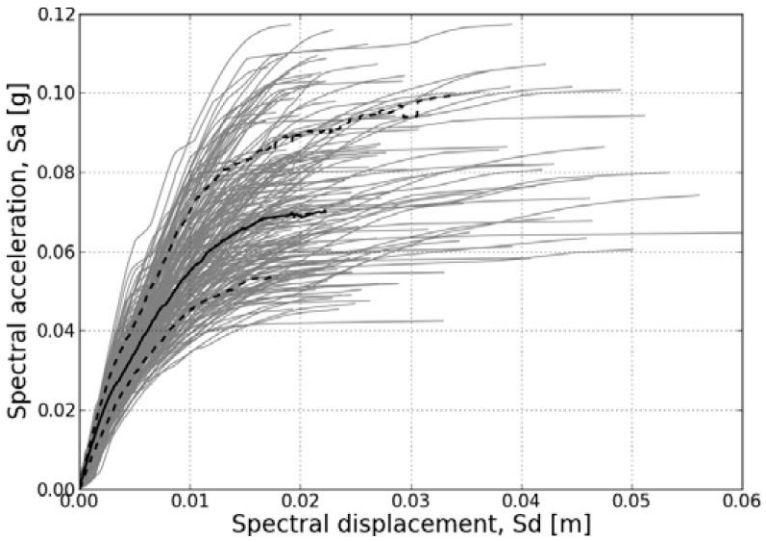

Figure 1 – Capacity Curves – Royal Monastery of Santa Maria de Poblet (Petromichelakis, Saloustros, & Pela, 2014)

The collapse capacity had a large variation while the variation of the elastic component of the capacity curve is low by comparison. A reference model was analyzed, where all parameters were average values of the ranges of the varied parameters. Comparing the mean and median capacity curve to the reference curve, the reference curve produced the most conservative results. This shows that one or more input parameter has an unsymmetrical influence on the structure's capacity. Unlike (Contrafatto, 2017), the damage grades denied based on damaged observed during lateral loading, in this case three damage grades were found. First, cracking near the key of the main nave and rotation of the external wall. Second, propagation of opening hinges, three in the main nave, three in the lateral aisle, and rotation of the pier in the main nave. Thirdly, collapse. These damage grades were used for a fragility assessment.

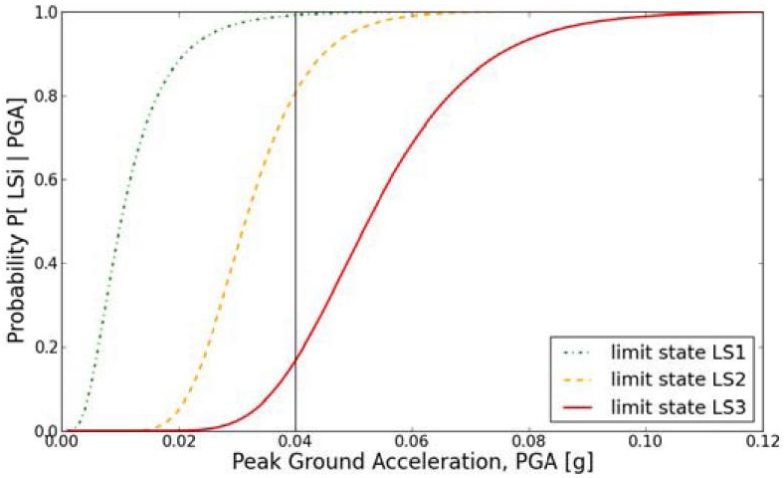

Figure 2 – Fragility Curves of – Royal Monastery of Santa Maria de Poblet (Petromichelakis, Saloustros, & Pela, 2014)

Concluding the structure having a low probability, 18%, of collapse for the earthquake demand (Petromichelakis, Saloustros, & Pela, 2014).

2.3.2 Vulnerability Assessment of Monumental Masonry Structures Including Uncertainty

A similar study was conducted by (Contrafatto, 2017) on the Santa Maria Del Mar Cathedral in Barcelona, Spain. Similar to the (Petromichelakis, Saloustros, & Pela, 2014) study, a two-dimensional model representing a typical bay was considered to determine the seismic response through pushover analysis. Contrafatto only considered three parameters for the uncertainty analysis compressive strength, tensile strength, and Young's modulus. The ranges were determined from previous studies on the Cathedral and according to (IMIT, 2009). The effect of the uncertainty of material properties was determined using a Monte Carlo simulation to generate a possible populations of material properties. The variability of the structural response was determined through nonlinear static analysis.

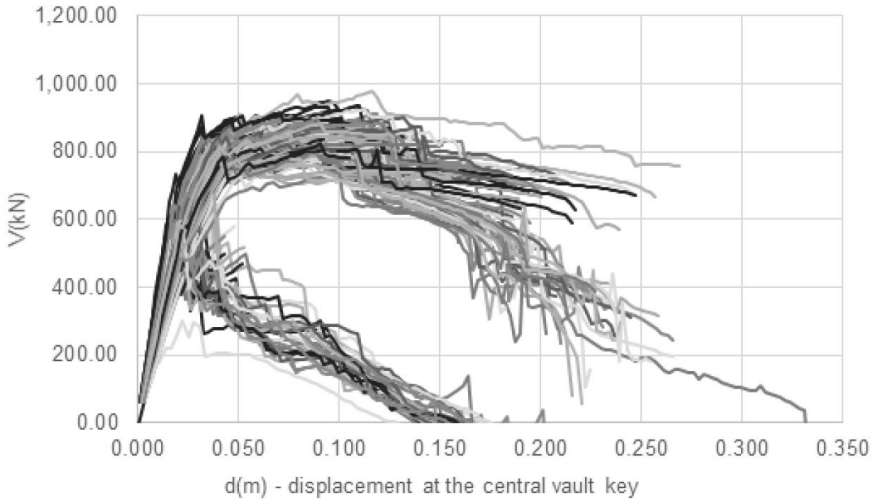

Figure 3 - Capacity Curves – Santa Maria Del Mar Cathedral (Contrafatto, 2017)

Unlike (Petromichelakis, Saloustros, & Pela, 2014), four damage grades were considered. These damage grades were determined using the mechanical approach (Lagomarsino & Giovinazzi, 2006). A fragility assessment was conducted to determine the probability of each damage grade in the event of an earthquake. There was significant variation found in the capacity of the Santa Maria Del Mar through the variation of the material mechanical properties. The important conclusion from this study was three different mechanisms found. Two global and one local mechanism. Both global and local mechanisms resulted in damage to the triangular buttress, upper part of the lateral vaults, and the base of the right buttress; with a probability of 100% from the fragility assessment.

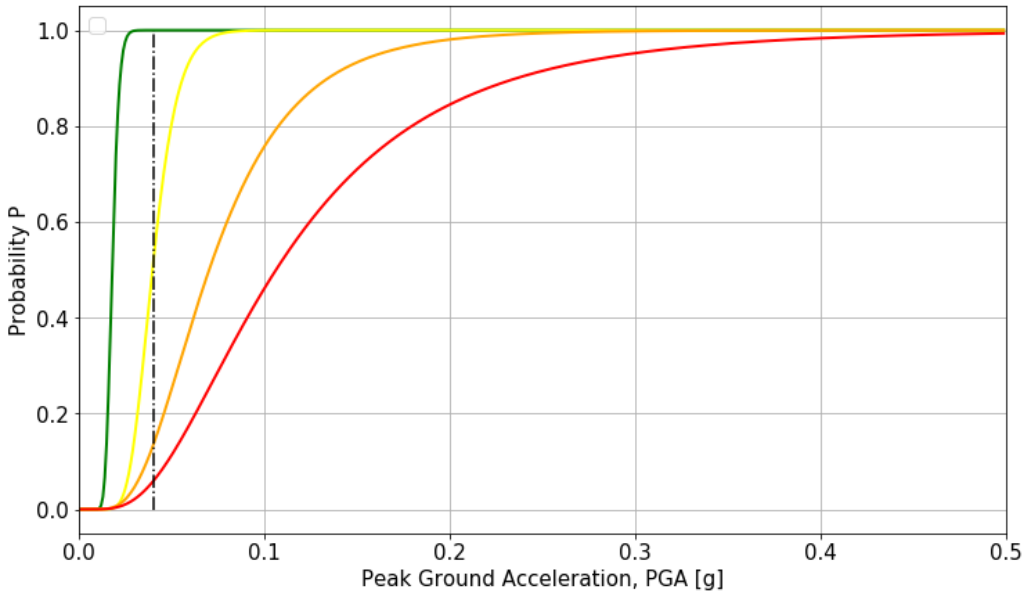

Figure 4 – Fragility Curve of Santa Maria Del Mar (Contrafatto, 2017)

The local mechanism also induces damage to the upper half of the right buttress. The expected earthquake damage was determined to be significant damage, while the probability of the collapse of the structure was derived to be low (Contrafatto, 2017).

2.3.3 Vulnerability Assessment of Masonry Churches Including Uncertainty

(Bitlloch, 2018) conducted another study on the Basilica de Santa Maria del Pi in Barcelona, Spain. A similar procedure to (Contrafatto, 2017) was considered. An equivalent plane-stress two-dimensional finite element model of a transversal bay was developed and calibrated to a three-dimensional model. Similar to Contrafatto three parameters were considered for the uncertainty analysis compressive strength, tensile strength, and Young's Modulus. There were no previous studies or testing available for the mechanical properties of the church, therefore, the ranges were determined according to Italian recommendations (IMIT, 2009). A Monte Carlo Simulation was then performed to generate a population of 200 material properties, which were analyzed using nonlinear static analysis, same as Contrafatto and Pertromichelakis et al. (Petromichelakis, Saloustros, & Pela, 2014). The N2 method was applied and adapted in this study. Unlike in the other studies, this study considered multiple control nodes since no strong conclusion was found in literature. The nodes considered shown in Figure 5 (a) key of the nave vault, (b) right spring of the nave vault, (c) the lower top-right corner of the right buttress, (d) the higher top-right corner of the right buttress, and (e) the higher-right point of the macroelement.

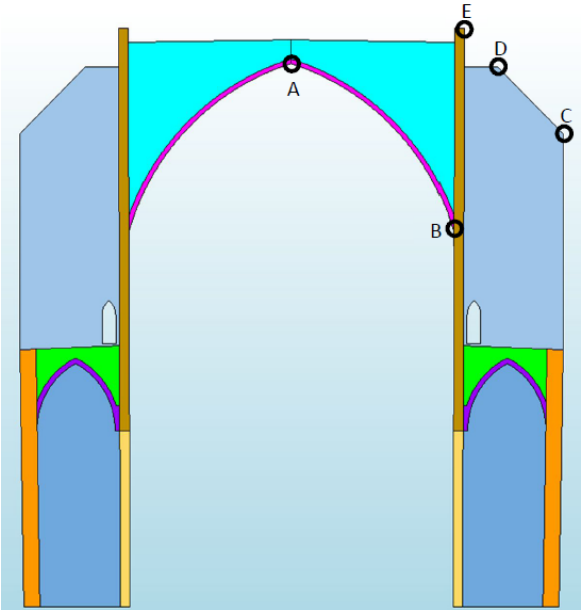

Figure 5 – Control Nodes Considered in the Application of the N2 Method – Santa Maria del Pi (Bitlloch, 2018)

The obtained capacity curves were idealized into bilinear curves. Difference damage grades were considered compared to the other two similar studies. In this study, three damage grades were determined from a literature review which can be related to grades 2 to 4 in the EMS-98 (European Seismologic Commission, 1998) and the three limit states of the Eurocode 8-1 (European Committee for Standardization, 2004). Finally, similar to (Contrafatto, 2017) and (Petromichelakis, Saloustros, & Pela, 2014) fragility curves were derived, in this study fragility curves for each of the control nodes were derived. Most of the curves were similar to one another. The highest probability of damage was obtained from the control node B at 10% probability of damage grade one, seen in Figure 6.

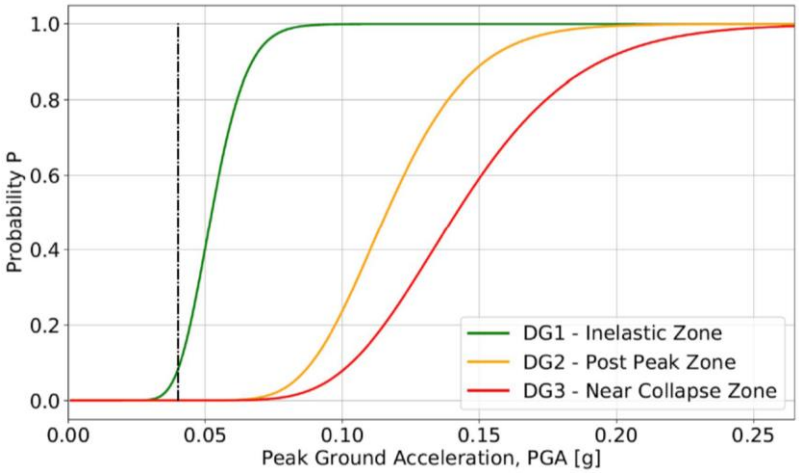

Figure 6 – Fragility Curves of Node B of Santa Maria del Pi (Bitlloch, 2018)

Second, node C with a probability of 5%. The other nodes the probability of any damage grade is negligible at 0.04 g peak ground acceleration.

3. CASE STUDY: MALLORCA CATHEDRAL

The site chosen for the analysis over the deration of this case study was the Mallorca Cathedral in Palma, Spain. The first stage of this study was a bibliographic research analysis which makes up the following sections describing the cathedral and the previous studies and analyses that have been conducted on the site.

3.1 Introduction and History

The Mallorca Cathedral is located in Palma, Spain, on the island of Mallorca. The Mallorca Island is east of the mainland of Spain and is the largest island of the Balearic Islands in the Mediterranean Sea, which can be seen in Figure 7.

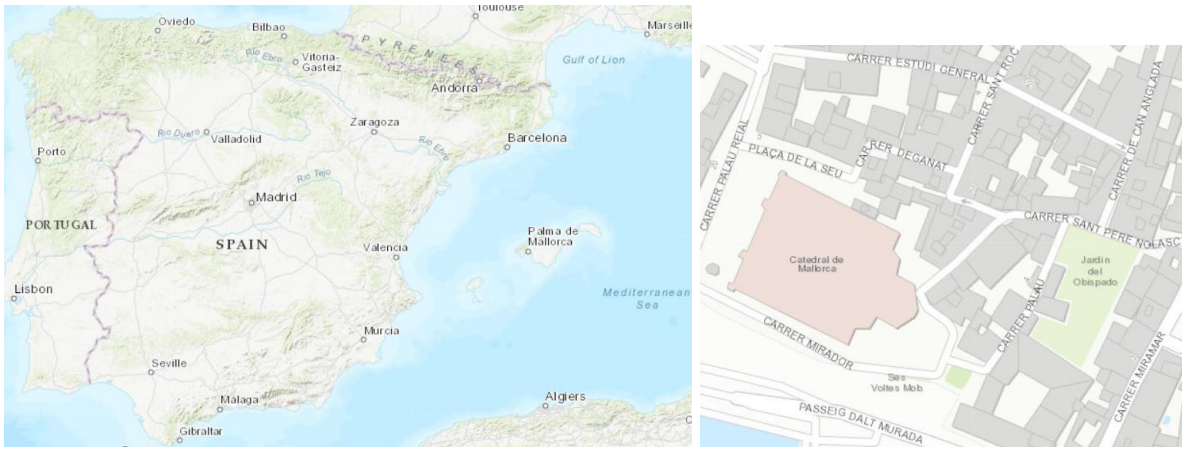

Figure 7 - Map of Spain and Mallorca Island (Esri, 2018)

The Mallorca Cathedral is of Gothic construction built during the XIII – XV century, which can be seen in Figure 8.

Figure 8 – Exterior View of Mallorca Cathedral (Trip Wolf, n.d.)

The construction of the cathedral began in 1306, with financial backing of King Jaume II, during the first insular dynasty reign. Construction of the cathedral was not completed until 1600, with a break in the construction from 1450 to 1560. The Trinity Chapel was the first element of the cathedral to be constructed, followed by the Real Chapel in 1330 and six lateral chapels that were completed by 1370. By 1374, the first bay of the nave was built. The second bay and two lateral chapels were constructed by 1385, while the west façade and adjacent chapel was constructed during the 14th century. The third bay and two lateral chapels on the north side were completed by 1406, while the forth bay was constructed during the 15th century. The fifth bay has an increased span, and therefore had an increased construction time. The bay and three chapels were completed by 1560. The next three bays were constructed quickly, in thirty years, this was because of financial support from Joan de Vich y Manrique. The construction of the Mallorca Cathedral was concluded with the west façade in 1601.

The cathedral went through a reconstruction phase from 1639 to 1851. The first important structural problem occurred in 1639, when numerous parts of the cathedral failed or had critical cracking. Therefore, the main nave and west façade were dismantled and rebuilt. On March 18th, 1660 there was an earthquake resulting in the failure of two arches and out-of-plane overturning of the west façade. In 1851 the west façade was dismantled, after an earthquake furthered its deterioration. Juan Peyronnet Baptist was the architect who designed the new façade. The new design was flamboyant neo-gothic style, which was very different from the old construction. The construction of the new façade was completed in 1888. After this phase there was a series of interventions, continuous repair work, and maintenance. The most significant of these activities was the restoration of the west and south facades (Elyamani, 2015).

3.2 Description

The Mallorca Cathedral is a great example of gothic architecture. The church has a length of 121m and is 55m wide. The Cathedral exhibits many of the features typical of the Catalan gothic style including high lateral naves, chapels between the buttresses, extremely slender octagonal piers, and a spacious interior. Typical sections of the Mallorca Cathedral can be seen below in Figure 9.

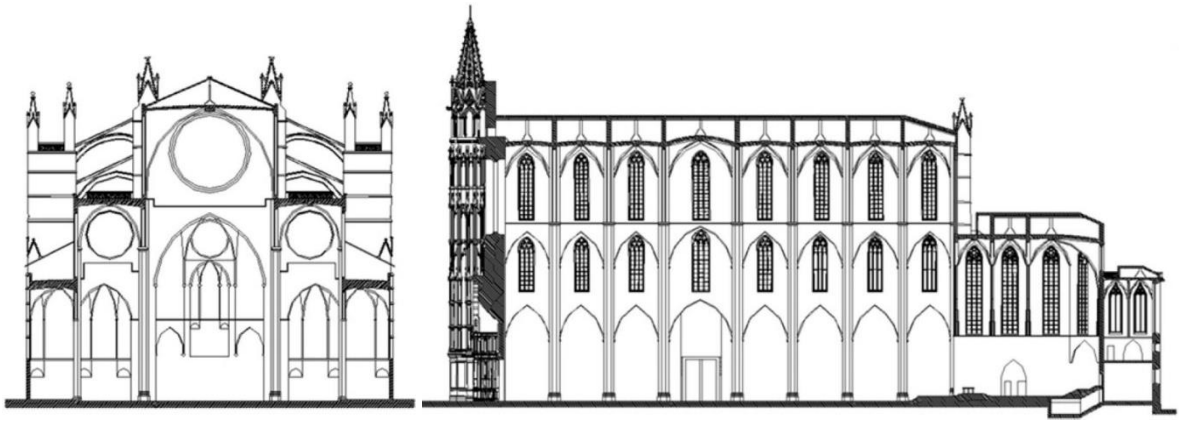

Figure 9 - Mallorca Cathedral - Sections (Roca, Cervera, Pela, Clemente, & Chiumenti, 2013)

The cathedral was constructed using limestone from local quarries. The columns have the highest slenderness ratio of all the gothic cathedrals in the world, with a height to width ratio of 14.6. Also, the cathedral has the second longest main nave at 77m, after the Girona Cathedral (Elyamani, 2015). The main nave has a free span of 17.8m and a height of 44m, with octagonal columns with diameters of 1.7m or 1.6m. While the lateral naves have a span of 8.75m and height of 29.4m (Pela, Bourgeois, Roca, Cervera, & Chiumenti, 2016). There are two main parts of the structure, first the oldest including the Royal Chapel and Hotel Trinity Chapel, located on the west side of the structure. Secondly, the main nave that consists of three parallel naves with lateral chapels between the buttresses. There are seven bays that make up the three parallel naves. This can be seen in the following floor plan of the Mallorca Cathedral, Figure 10.

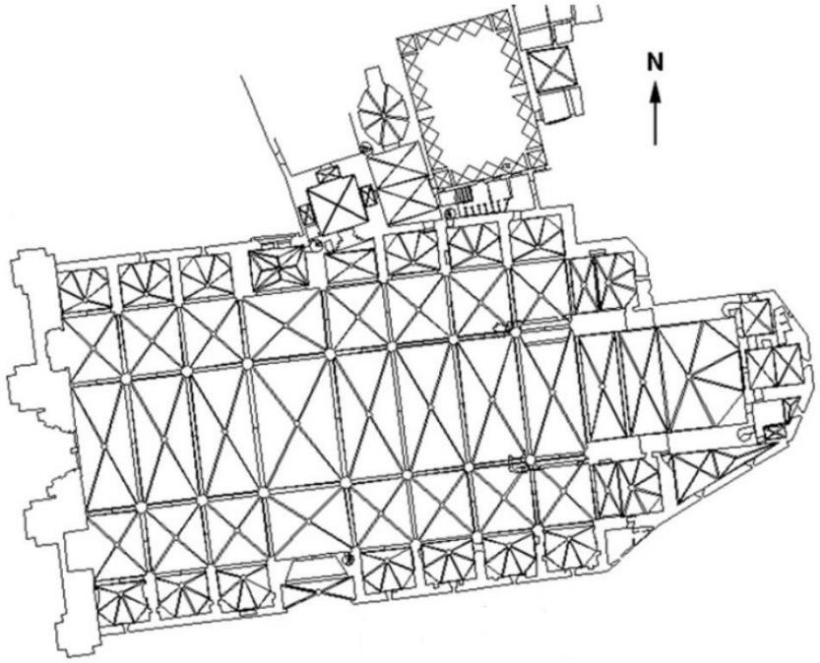

Figure 10 - Mallorca Cathedral - Floor Plan (Roca, Cervera, Pela, Clemente, & Chiumenti, 2013)

3.3 Previous Studies

There have been several studies performed on the Mallorca Cathedral since the beginning of the 20th century whose focuses include historical research, inspection of structural elements and the underlying soil, and structural assessments.

The structural assessments in some cases included graphic-static analyses of a typical bay of the Cathedral. Joan Rubió conducted a study (Rubió, 1912) and found a thrust line through the section of the main nave arch, flying arches, and buttress. This thrust line can be seen below in Figure 11 (Rubió, 1912).

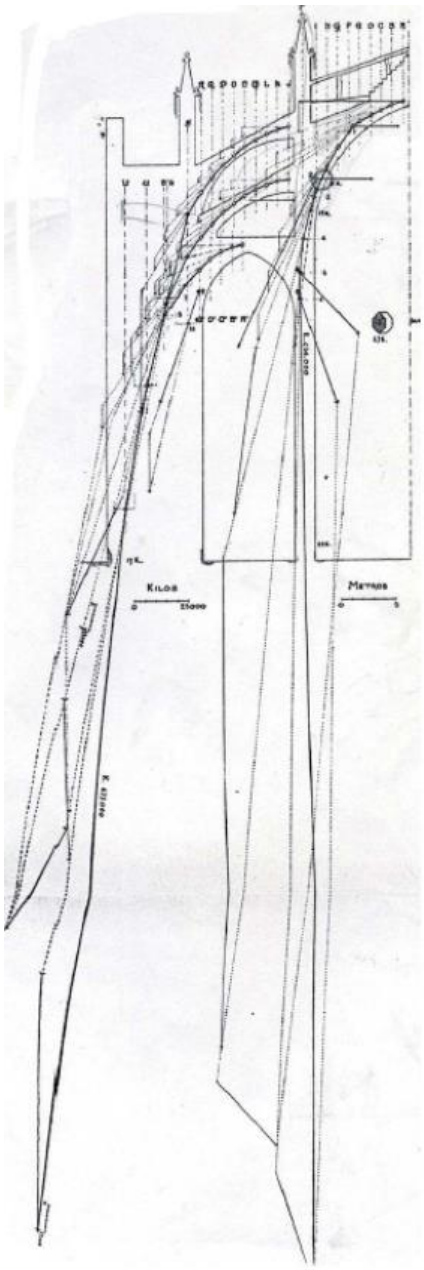

Figure 11 – Thrust Line through Mallorca Cathedral (Rubió, 1912)

A confirmation study was done by Maynou in 2001 (Maynou, 2001), modernizing the work of (Rubió, 1912) where an automated implementation of the graphic-statics method was preformed. This found multiple thrust lines confirming the need for the dead weight above the main nave and vaults for the stability of the structure. The generated thrust lines can be seen in Figure 12, the red thrust lines highlight the outer most boundaries (Maynou, 2001).

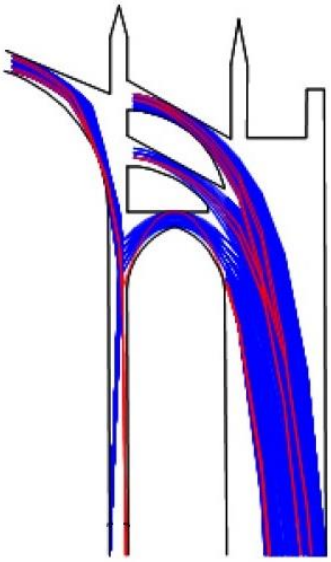

Figure 12 – Automatically Generated Thrust Lines (Maynou, 2001)

A photo-elasticity study was completed by Mark in 1982 (Mark, 1982). A typical bay was modelled, and scaled gravity and wind loads were applied. A pattern of light was passed through the model resulting in a distribution of internal stresses that could be qualitatively interpreted. A uniform state of compression in the columns under gravity loads was found during this study, as seen in Figure 13 (Mark, 1982).

Figure 13 – Photo-Elastic Analysis (Mark, 1982)

Several numerical analyses were completed by multiple researchers, most considering only a typical bay of the cathedral. All of these studies used deterministic properties. Firstly, Salas (Salas, 2002) performed finite element modelling with an isotropic damage model and generalized matrix formulation. A typical bay was considered using linear and nonlinear analyses. First, the self-weight of the cathedral was considered using the theoretical undeformed geometry and the actual deformed geometry. The maximum compressive strength, deflection of the main nave arch and horizontal displacement of the top of the column was compared. There was no significant difference between the two. Linear and nonlinear analyses were also compared, resulting in no significant increase in stress or displacement when using nonlinear analysis. Both modelling methodologies, Finite Element Modelling and the Generalize Matrix Formulation Method, yielded the same results. The safety margin of the Cathedral under self-weight was also tested, yielding in collapse under 1.7 times the amount of the structure's self-weight. Specific parts of the Cathedral were removed to determine the effect on the capacity under the self-weight. First the flying arches resulting in collapse at 0.7 times self-weight, overweight with a collapse at 0.9 times self-weight, and finally both the flying arches and overweight were removed resulting in a collapse at 1.6 times self-weight. Wind and earthquake analyses were also performed. These yielded similar collapse mechanisms. These collapse mechanisms presented hinges in the main nave arch, upper and lower flying arches, lateral nave vaults, and the base of the columns and buttresses, which can be seen in the Figure 14, below (Salas, 2002).

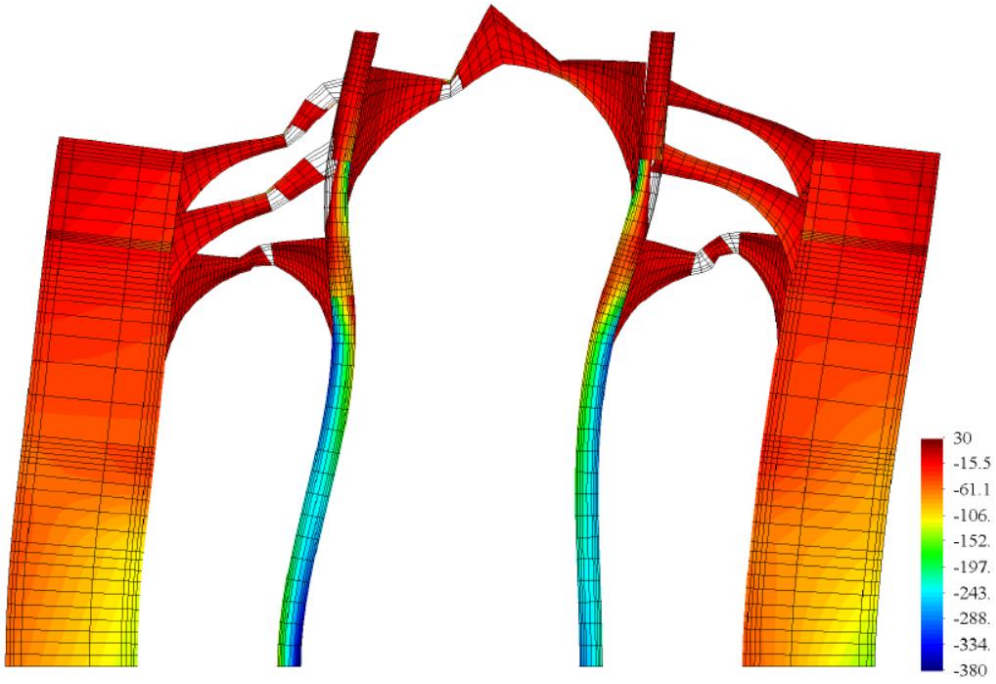

Figure 14 – Deformed Shape and Stress Distribution at Collapse due to Wind Loading (Salas, 2002)

Clemente (Clemente, 2006) conducted a study on the Mallorca Cathedral that used both distributed and localized damage models, in both two and three-dimensions. Multiple analyses were performed considering different loading conditions. The loading conditions for each the individual analyses were

self-weight, self-weight and the construction process, creep deformation, and seismic loads. Under the self-weight the load factor was determined to be 2 before collapse, while using the localized damage model a load factor of 2.15 was reached. When considering the construction process an increase of the horizontal displacement of 1.09cm was found. As well as more damage at the top of the column, flying arches, and vaults. The next analysis considered was completed to investigate the effect of creep. Considering creep concluded there was a horizontal displacement of 12 cm at the top of the column, which is similar to the actual displacement in the Cathedral, and no change in the collapse mechanism was observed. A sensitivity analysis was then completed with the tensile strength, compressive strength, and tensile fracture energy. The collapse load factor decreased as the tensile strength decreased. A linear relationship between compressive strength and load factor was observed. When the tensile fracture energy was low the structure could not hold its self-weight (Clemente, 2006).

Roca et al. (Roca, Cervera, Pela, Clemente, & Chiumenti, 2013) continued and refined Clemente's study (Clemente, 2006) considering the influence of the construction process and long-term deformation currently exhibited on the Mallorca Cathedral. The numerical modelling was based on continuum damage mechanics theory. With mechanical damage and long-term viscous effects considered. To determine the effects the construction process, and the damage was improved using crack tracking. A viscoelastic model was used to account for the creep. While tension-compression damage model was used, so different damage criteria for tension and compression could be considered. To determine the effect of the construction process, a sequential analysis was completed with a typical bay of the Cathedral. As determined through historical investigation the steps of the construction process were simulated. This resulted in three analyses, first the lower part of the finite element analysis activated the buttress, lateral vault, and pier, secondly, the entire bay is activated in the analysis, and finally, the effects of creep were considered. In the first analysis, it was determined the intermediate state was withheld by the structure throughout the construction process. The intermediate state was only made possible because of the tensile strength of the masonry, cancelling out the unbalanced thrust from the lateral vaults, as no braces or ties were used in the construction. The deformed shape and tensile damage developed during this stage is seen in Figure 15 (a) and (b) respectively. The second analysis determined issues may have developed during the construction during the first phase. The deformation of the pier increases due to initial creep. This would have required some corrections to made at this stage of the construction. The deformation and tensile damage concluded from this analysis is shown in Figure 15 (c) and (d).

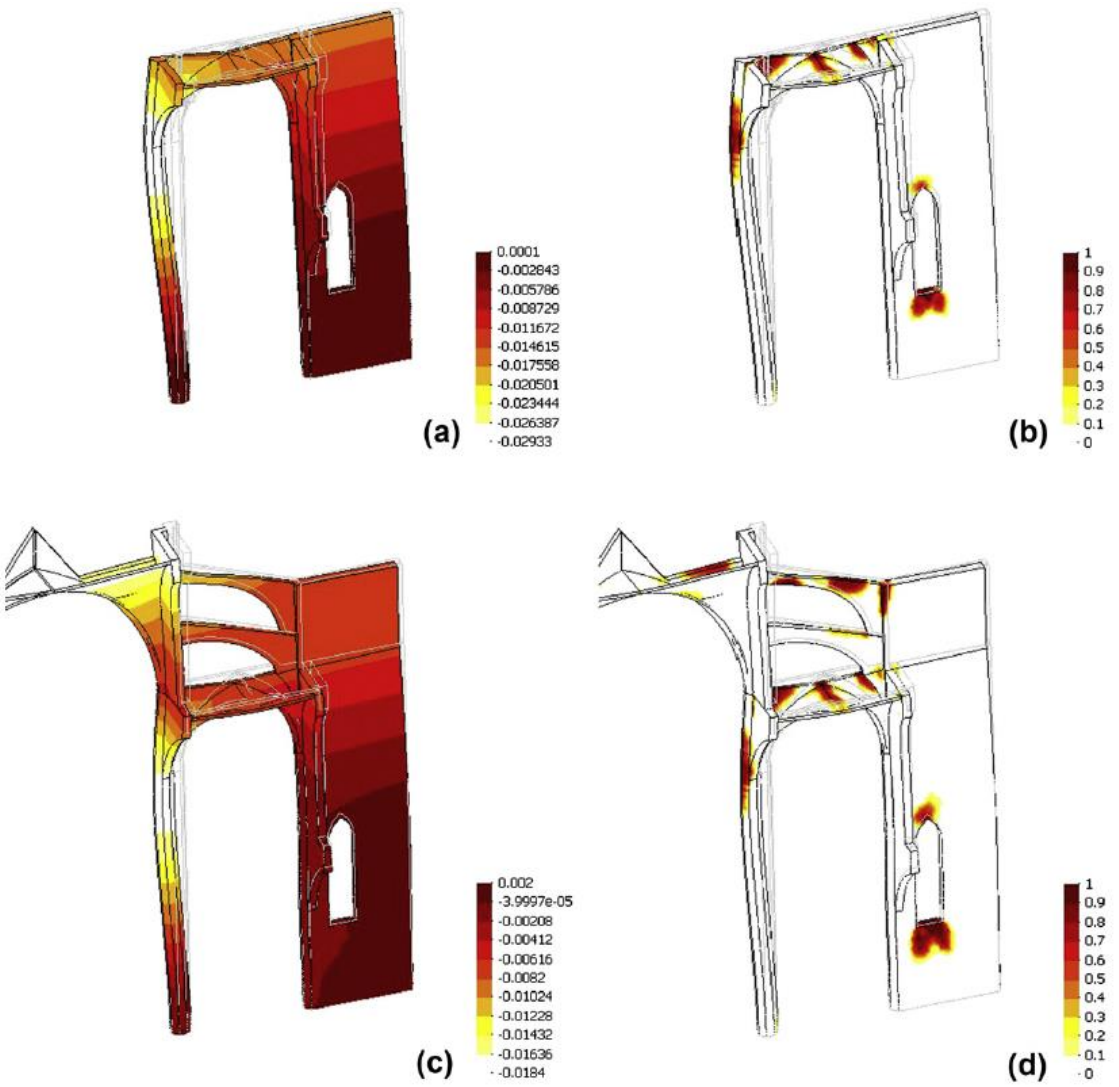

Figure 15 – Deformed Shape and Tensile Damage in Construction Analysis (a) First Stage Deformed Shape (b) First Stage Tensile Damage (c) Second Stage Deformed Shape (d) Second Stage Tensile Damage (Roca, Cervera, Pela, Clemente, & Chiumenti, 2013)

The introduction of creep to the analysis of the Mallorca Cathedral introduced two parameters retardation time and participation ratio. The time was assumed in pseudo-time units and the retardation time was arbitrarily assumed as 50-time units. Two values for participation ratio were considered: 0.875 and 0.975. The first producing results similar to the present deformation measured in the Cathedral, which can be observed in Figure 16.

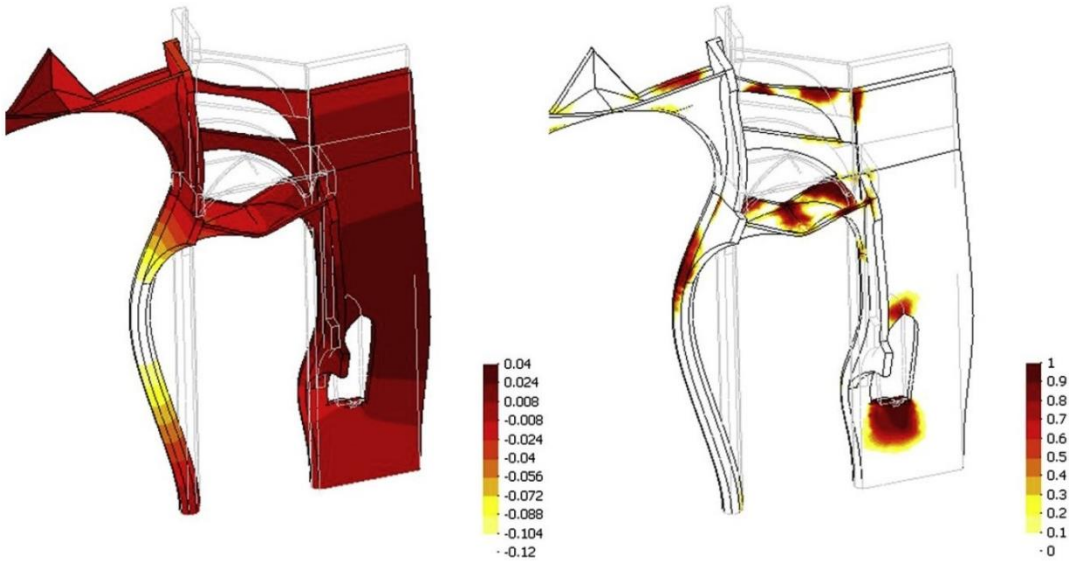

Figure 16 - Simulation of Long Term Deformation Including Effects of Construction Process - Deformed Shape (left) and Tensile Damage (right) (Roca, Cervera, Pela, Clemente, & Chiumenti, 2013)

Therefore, the long-term deformation and nonlinear geometric effects had a significant role in the behaviour of the structure. Finally, a seismic load analysis with an equivalent two-dimensional model was also performed on the representative bay with the use of localized damage model. Using this model, the capacity increased, three exclusion radius values were used, each increased the capacity as the value increased. This also resulted in a more realistic representation of the cracks and collapse mechanism.

Martinez (Martinez, 2007) developed a seismic assessment methodology and applied it to the Mallorca Cathedral. A three-dimensional finite element model was updated using dynamic identification testing, updating the Young's Modulus. Pushover analyses were performed on five macro-elements; typical bay, transept bay, triumphal arch, west façade and longitudinal bay. The highest amount of damage was experienced in the longitudinal bay, with a damage level of D3 using the methodology proposed by (Martinez, 2007).

Roca et al. (Roca, Vacas, Cuzzila, Murcia-Delso, & Das, 2009) performed a nonlinear analysis considering gravity and seismic loads with a tension-compression distributed damage model on the Mallorca Cathedral. This resulted in a similar collapse mechanism to a past study by (Clemente, 2006). Two load patterns were also considered proportional to mass and proportional to the first mode of vibration. The second load pattern yielded a higher capacity compared to the first. A sensitivity analysis of the tensile strength was also completed during this study. When the tensile strength was reduced the capacity of the structure was reduced. Finally, the capacity spectrum method was applied to the Mallorca Cathedral. This yielded acceptable performance and limited damage (Roca, Vacas, Cuzzila, Murcia-Delso, & Das, 2009).

Pela et al. (Pela, Bourgeois, Roca, Cervera, & Chiumenti, 2016) performed a numerical analysis study which considered the use of ties during the construction process. During an inspection evidence was found of iron ties used during construction which were later removed. Therefore, a study considering adding ties during the initial construction and removing the ties after the construction, as seen in the Figure 17, was conducted.

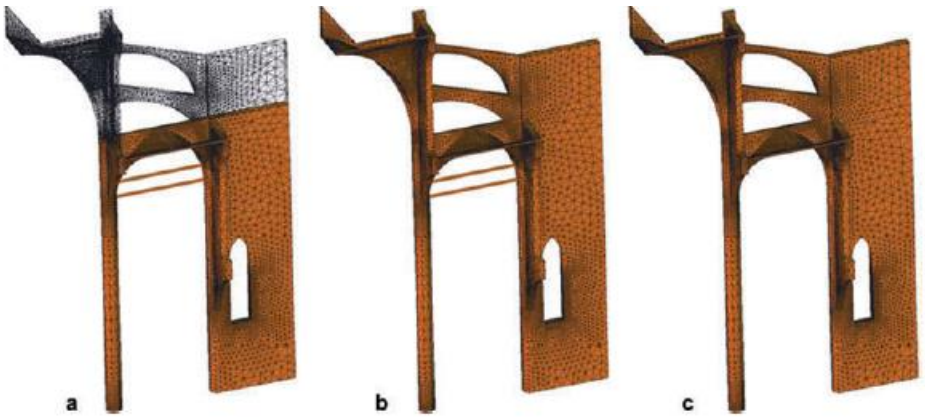

Figure 17 - Finite Element Model of Study of the Effect of Ties Used During the Construction Process (a) Initial Construction with Ties (b) Complete Construction (c) Removal of Ties (Pela, Bourgeois, Roca, Cervera, & Chiumenti, 2016)

This analysis was completed through numerical modelling with material nonlinearity and geometrical nonlinearity. Through this analysis it was found that the ties improved the performance of the structure during construction. The ties balanced the thrust from the lateral vaults, reducing the displacement of the column. This can be seen in Figure 18, comparing the deformed shape and tensile damage with and without ties during the first stage of the construction process. This included only the column, lateral vault, and buttress.

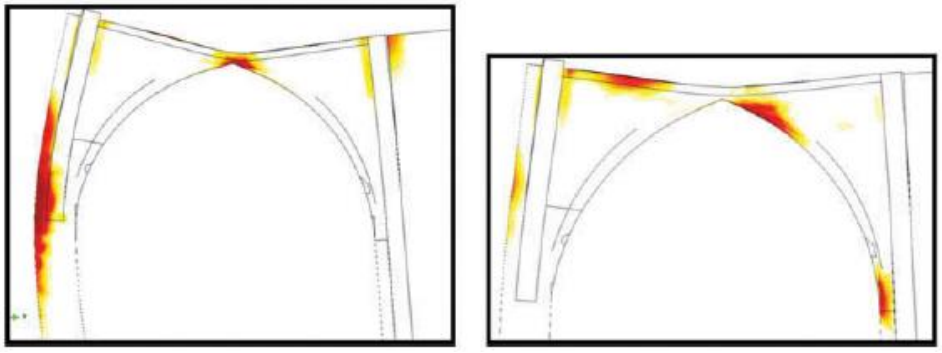

Figure 18 – Deformed Shape and Tensile Damage of Lateral Vault Without the Use of Ties During Construction (Left) and With Ties (Right) (Pela, Bourgeois, Roca, Cervera, & Chiumenti, 2016)

As seen in Figure 18, the use of ties in the initial construction phase significantly changes the initial damage experienced by the structure. The long-term damage was also studied to determine the effect

of the ties. It was concluded that there was a reduction in displacement of the columns with the implementation of the ties during construction. The ties also modified the crack pattern, with significant reduction in the column but considerable increase in the arches and vaults (Pela, Bourgeois, Roca, Cervera, & Chiumenti, 2016).

(Elyamani, 2015) conducted a seismic safety assessment of the Mallorca Cathedral. To begin Ambient Vibration Testing was completed to identify the natural frequency, mode shape, and damping ratios. Continuous monitoring was then implemented to measure and record accelerations 24 hours a day. The natural frequencies and mode shapes obtained from the testing was used to update the three-dimensional finite element model. Using this model, a seismic assessment was completed. Pushover analyses were completed in four directions defined as x, y, in both the positive and negative directions. The strongest direction being the negative y-direction with a capacity of 0.141g, the cracking pattern at this collapse and the sequence in which the cracks form can be seen in Figure 19.

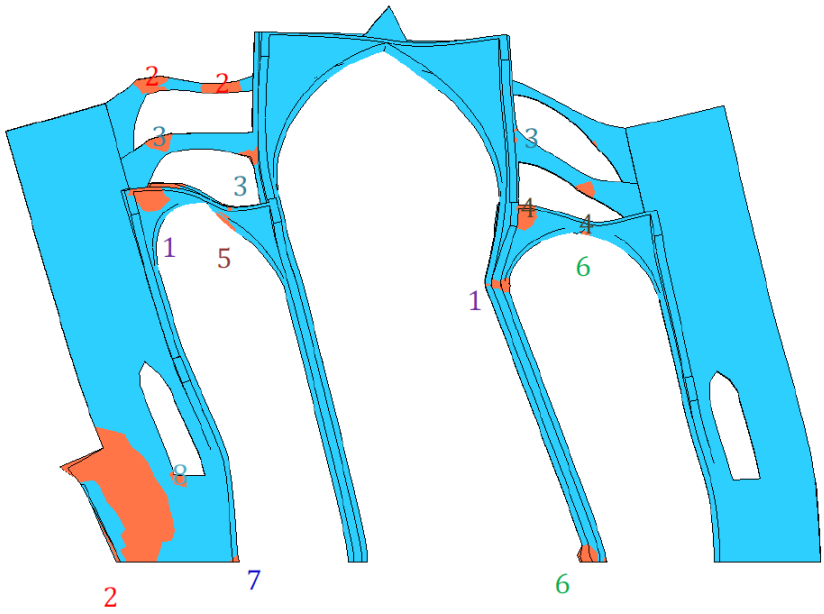

Figure 19 - Cracking Pattern and Sequence of Cracking at Collapse During Pushover Analysis in the Negative Y-Direction (Elyamani, 2015)

A sensitivity analysis was also conducted in regard to the tensile strength, compressive strength, ultimate crack strain, and modulus of elasticity. With regards to the tensile strength when reduced by 24% the capacity reduced by half, while an increase of 24% tensile strength the capacity almost doubled. A linear correlation between the tensile strength and capacity was concluded. In terms of compressive strength, decreasing the compressive strength had considerably more effect than increasing it. When the ultimate crack strain was reduced by an order of one the capacity was reduced by about 60% with a brittle behaviour. While when the ultimate crack stain was increased one to three orders only a slight increase in the capacity and elastic-perfect plastic behaviour was experienced. In terms of modulus of elasticity with a reduction in capacity of 17% and 37% was determined when reducing the modulus of

elasticity to half and a quarter, respectively. Also, nonlinear behaviour was experienced earlier with the reduction of the modulus of elasticity. A kinematic analysis was completed considering two collapse mechanisms, overturning of the west façade and east façade in both positive and negative directions. With the positive direction having a larger capacity than the negative direction. These results were near the pushover capacity. Lastly, a nonlinear dynamic analysis was performed on the Cathedral. In this analysis two approaches were considered to represent the seismic action; artificial accelerations and recorded accelerations. Similar spectra were obtained from both methods. Seismic actions were considered in both the longitudinal and transversal directions. In both directions the seismic actions were resisted without collapse of the structure. In the longitudinal direction, the points with peak displacements were the same as the pushover analyses in the positive and negative x-directions. The damage patterns at maximum displacement experienced the same scale as the pushover analyses. Lower values were obtained than the pushover analyses because a lower maximum resisted load was experienced. The damage pattern found at the maximum negative and maximum positive displacements can be seen in Figure 20 and Figure 21, respectively.

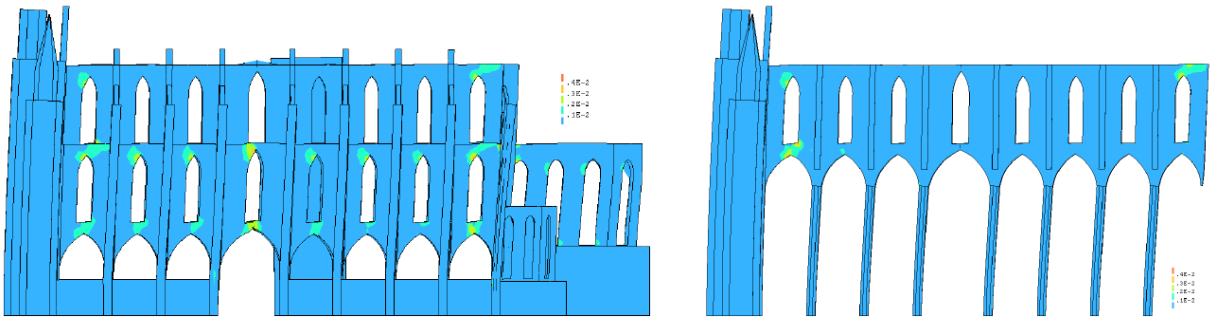

Figure 20 – Damage Pattern of Maximum Principal Strain with Deformed Shape at Maximum Negative Displacement During Nonlinear Dynamic Analysis in Longitudinal Direction (Elyamani, 2015)

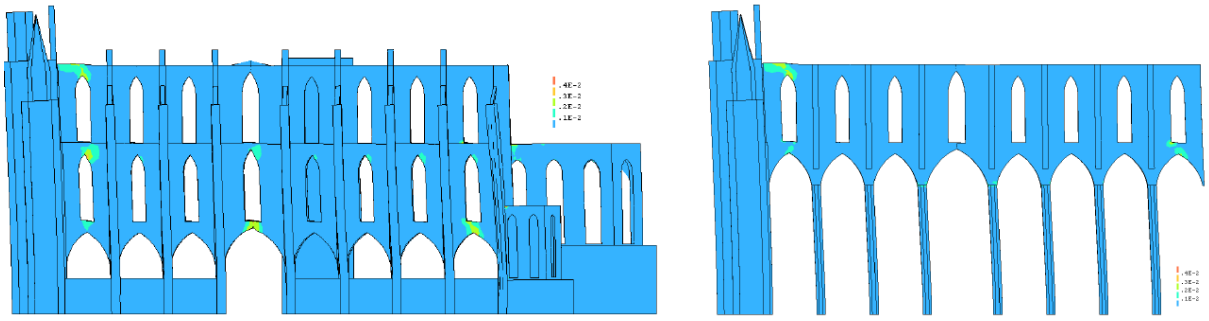

Figure 21 - Damage Pattern of Maximum Principal Strain with Deformed Shape at Maximum Positive Displacement During Nonlinear Dynamic Analysis in Longitudinal Direction (Elyamani, 2015)

In terms of the transversal direction, the load experienced in the nonlinear dynamic analysis was much lower than the resistance found in the pushover analyses in the positive and negative y-directions, 31% and 57% less, respectively. Figure 22 shows the obtained damage pattern and deformed shape at the maximum negative and positive displacements.

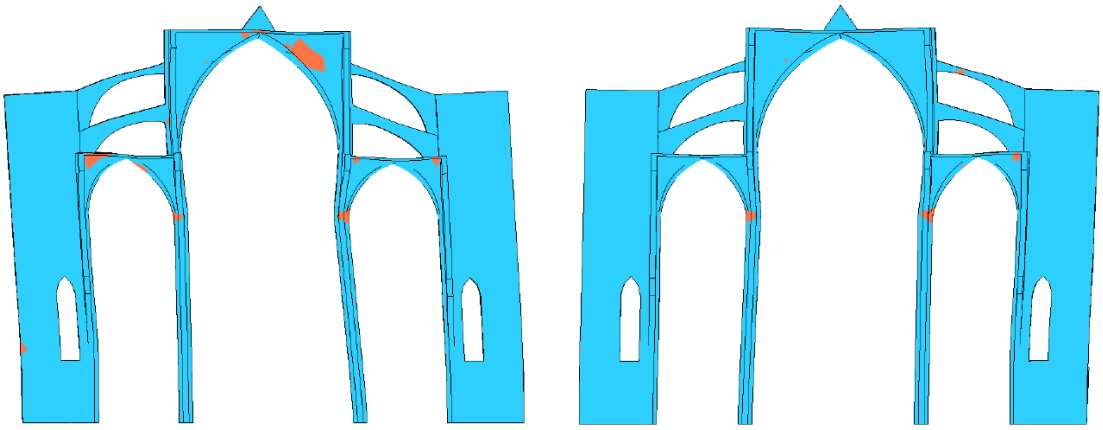

(a) (b)

Figure 22 – Damage Pattern of Maximum Principal Strain with Deformed Shape During Nonlinear Dynamic Analysis in Transversal Direction (a) Maximum Negative Displacement (b) Maximum Positive Displacement (Elyamani, 2015)

To evaluate the seismic performance of the Mallorca Cathedra Eylamani (Elyamani, 2015) considered the N2 method. 64 performance points, two seismic codes, and two return periods were considered for this evaluation. All points were determined to have sufficient seismic capacity. Therefore, it was concluded, no seismic strengthening necessary but repair of cracks and regular maintenance to be worthwhile (Elyamani, 2015).

Monitoring of the Mallorca Cathedral has been completed throughout the years. Static monitoring was conducted from 2003 to 2008 by (Gonzalez & Roca, 2008) monitoring crack widths, tilts, and convergences. This study concluded the crack opening the fastest had a rate of approximately 10 mm/century located between the sixth vault and supporting arch. Possibly because the west façade is continuing to tilt out-of-plane. The rest of the cracks were determined to have an opening rate of 2 mm/century or less (Gonzalez & Roca, 2008).

(Boromeo, 2010) processed recordings from dynamic monitoring to study the effect of environmental actions on the dynamic behaviour, showing the natural frequencies is dependent on the environmental actions. Increased temperature resulted in an increase in natural frequencies, while an increase in humidity or wind velocity resulted in a decrease in the natural frequencies (Boromeo, 2010).

4. NUMERICAL MODEL

Throughout this study a two-dimensional model was considered to reduce computational time during the simulations. In this section the analysis was completed with deterministic properties to calibrate the finite element model to the study by (Roca, Cervera, Pela, Clemente, & Chiumenti, 2013). The geometry, and all properties of the finite element model are discussed in the following section. The calibration process to a previous study (Roca, Cervera, Pela, Clemente, & Chiumenti, 2013) using nonlinear static analyses and the results from analyzing this model is presented in the subsequent sections.

4.1 Finite Element Model

Due to the repetitive nature of the bays in the Mallorca Cathedral a typical bay was considered for the numerical modelling for a representative study of the in-plane response of the structure in the transversal direction. The two-dimensional model was analyzed using the software DIANA FEA version 10.2. A two-dimensional model was calibrated to simulate the three-dimensional response using varying thicknesses and densities. This can be seen in the following figure, Figure 23. The geometry was obtained from existing geometrical survey completed by (Roca, Cervera, Pela, Clemente, & Chiumenti, 2013).

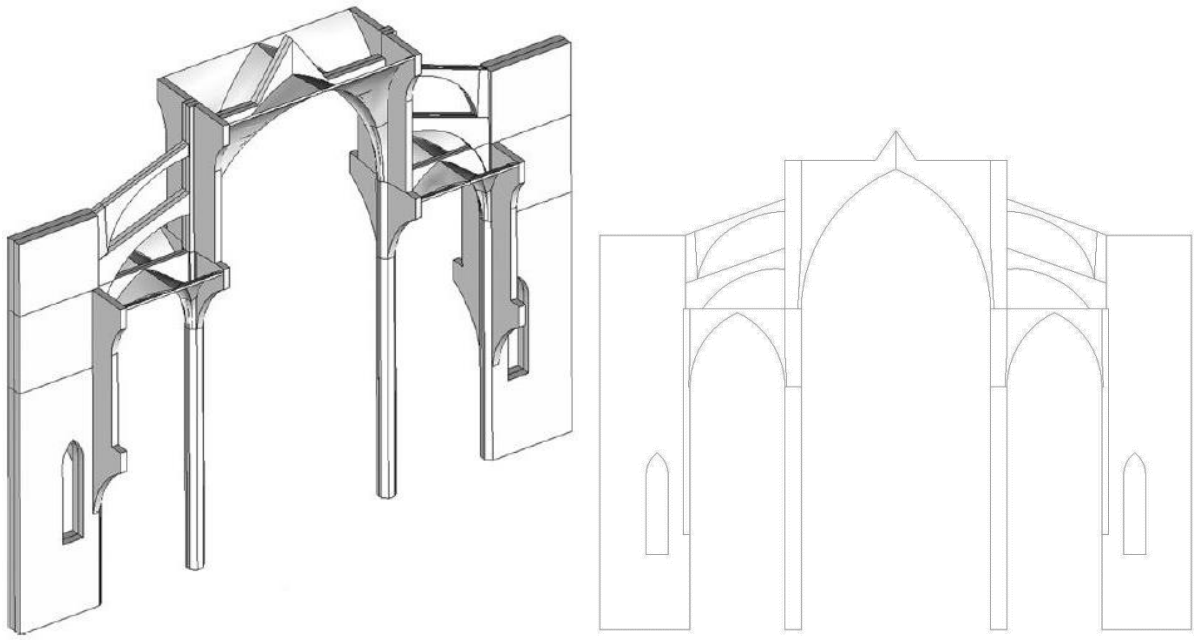

(a) (b)

Figure 23 – (a) Three-Dimensional Model Finite Element Model (Roca, Cervera, Pela, Clemente, & Chiumenti, 2013) (b) Two-Dimensional Model Finite Element Model

To begin the numerical modelling process only one quarter of the bay was considered. This model was broken up into eight different components. These different sections can be seen in Figure 24 below, these parts were used to simulate the change in thicknesses and mechanical properties throughout the

three-dimensional model. These also allow for different material properties to be assigned to the different parts of the structure, and the ability to account for different strengths for different materials throughout the cathedral.

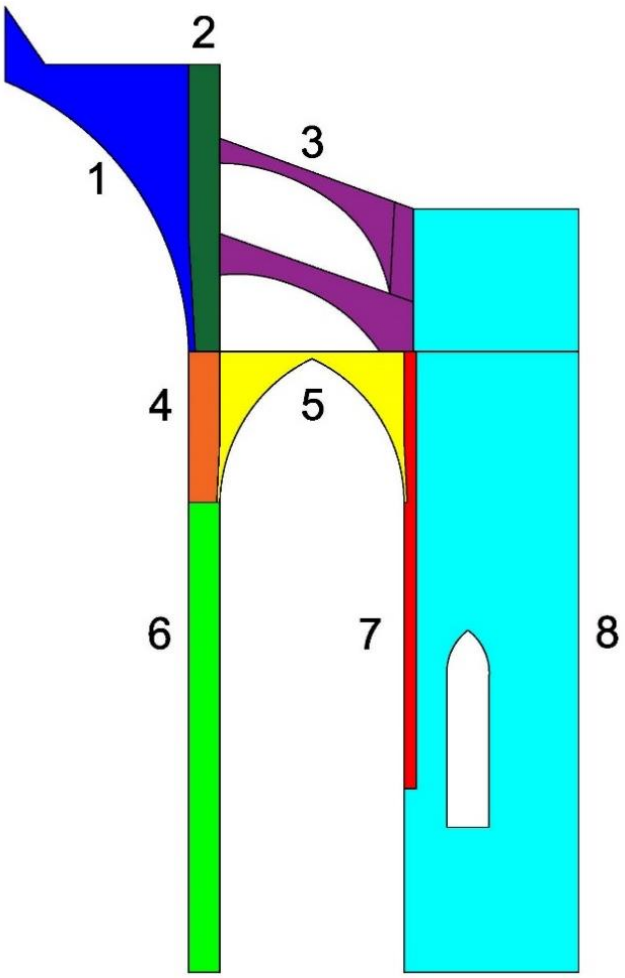

Element Number	Structural Element
1	Central Vault
2	Clerestory
3	Flying Arches
4	Column/Clerestory
5	Lateral Vault
6	Column
7	Lateral Clerestory
8	Buttress

Figure 24 – Structural Elements of 2D Model

The material properties and thicknesses were developed by (Roca, Cervera, Pela, Clemente, & Chiumenti, 2013), where a study was conducted on the construction process and existing deformation which were considered on the finite element model that was constructed. A common material was assumed for the buttress, vault, and clerestory. While the mechanical properties for columns and flying arches were grouped together and assigned higher values compared to the other categories. This is due to the columns monolithic character and the high-quality stone used in their construction (Elyamani, 2015). The mechanical properties of these components can be seen in Table 3.

Table 3 - Mechanical Properties from (Roca, Cervera, Pela, Clemente, & Chiumenti, 2013)

Component	γ [kg/m^3]	E [MPa]	υ	f^+[MPa]	f^-[MPa]	G_f^+[J/m^2]	G_f^-[J/m^2]
Buttress, Vault, Clerestory	2,100	2,000	0.2	0.10	2.00	100	40,000
Column, Flying Arch	2,400	8,000	0.2	0.40	8.00	100	40,000

While the thicknesses assumed for the components are provided in Table 4.

Table 4 - Thicknesses Used in Two-Dimensional Model (Roca, Cervera, Pela, Clemente, & Chiumenti, 2013)

Component	Thickness [m]
Central Vault	1.53
Clerestory	3.44
Flying Arches	0.90
Column/Clerestory	2.80
Lateral Vault	0.97
Column	1.24
Lateral Clerestory	2.71

After the mechanical properties were defined the next step in the modelling process is generating the mesh. Regular plane-stress elements were considered in order to be able to modify the thickness of each of the components to simulate the differences in stiffness experienced in three-dimensions. The tensile behaviour of the bay was assumed to be exponential, while the compressive behaviour was assumed parabolic, as demonstrated in the following graph.

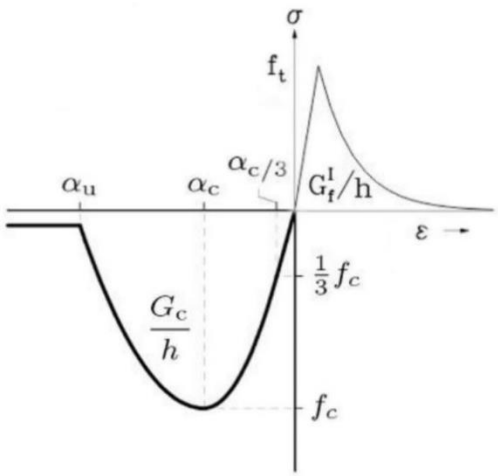

Figure 25 – Assumed Compression and Tension Behaviour

The rotating total-strain crack model was used for the nonlinear structural analysis. The numerical analyses were performed using the finite element software DIANA FEA. Triangular three node elements, T6MEM (Figure 26), were considered for this model because of the number of curves throughout the bay, reducing the tendency of the mesh to distort.

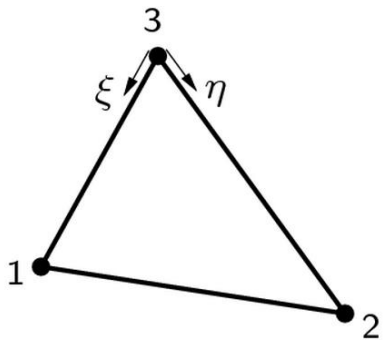

Figure 26 - Triangular Three Node Elements (DIANA FEA, 2017)

To begin the element size was considered to be 0.2 m throughout the model resulting in 51,098 elements. This resulted in the analysis taking an exorbitant amount of time. It was then concluded the mesh size needed to be refined to reduce the computational time, while not compromising the quality of the results. Therefore, a sensitivity analysis considering the element size of the mesh was conducted through pushover analyses. The relative displacement throughout these analyses was taken from the top of the interior right column, this point was chosen as it was the point used in the study by (Roca, Cervera, Pela, Clemente, & Chiumenti, 2013) to allow for a comparison of results to the study, presented in the next section. The overall mesh size of 0.2m was considered consistent throughout to ensure detail of the damage at the edges of the shapes was captured. Two mesh sizes were changed, the face of the buttress and the face of the main vault. These are the largest shapes, therefore, consists of the most number of elements. The element size of the face of the buttress was tested with a size between 0.2m

to 0.8m. While element size of face of the main vault between 0.2m and 0.4m was considered. This analysis can be seen in the following graph, Figure 27.

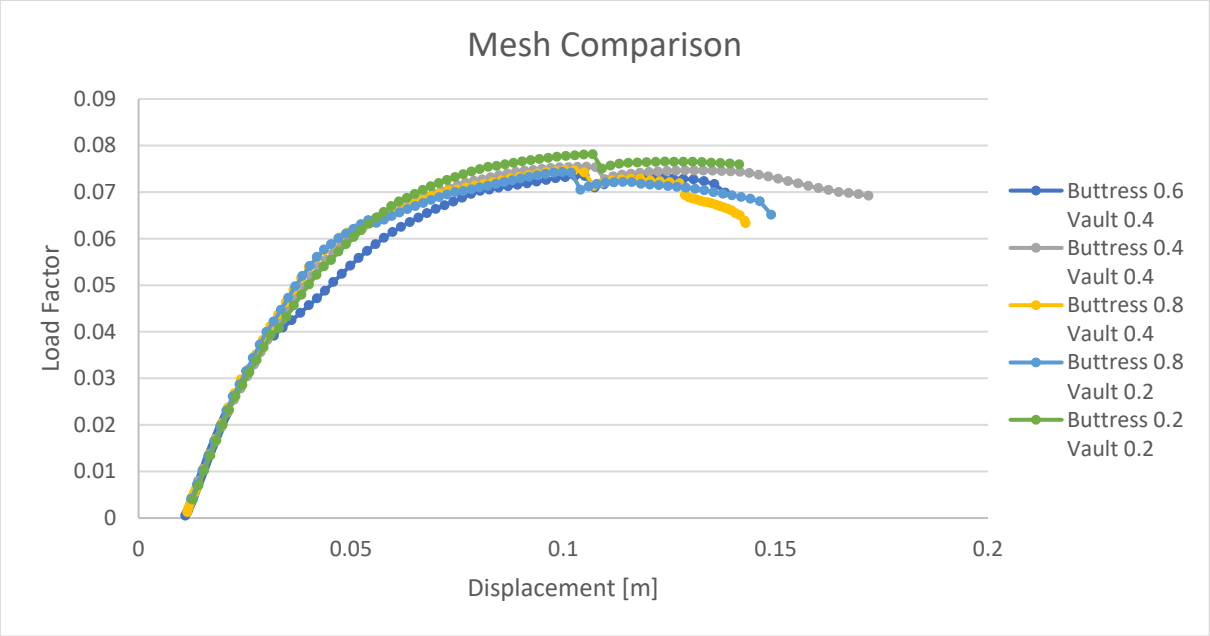

Figure 27 – Capacity Curve Comparison - Element Sizes Mesh

The mesh with the closest capacity curve to the original 0.2m mesh was the mesh with the face of the buttress and main vault having an element size of 0.4m.

The final mesh consisted of 27,144 triangular three node elements (T6MEM). The two meshes are shown below for comparison, in Figure 28 and Figure 29.

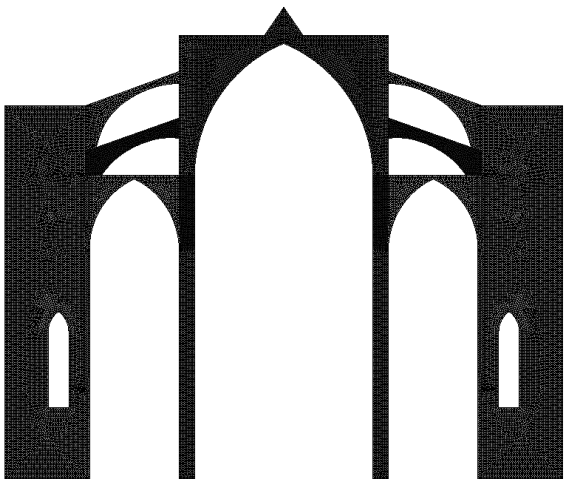

Figure 28 - Initial Finite Element Model Mesh

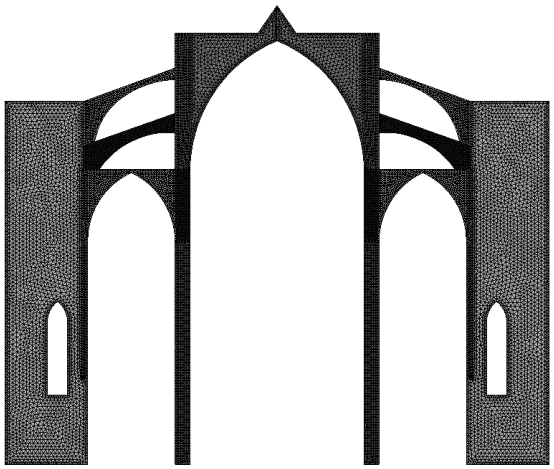

Figure 29 - Final Finite Element Model Mesh

Another comparison of the capacity curve can be seen in the figure below, Figure 30, this allows for an easier comparison of the initial and final mesh, without the other considered meshes.

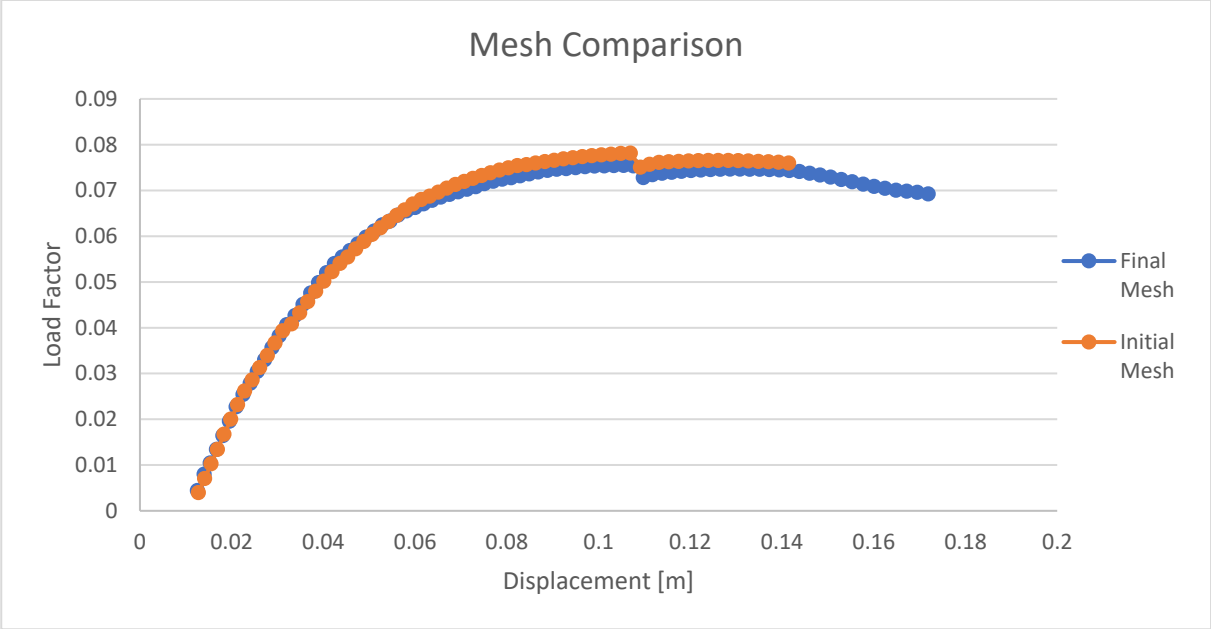

Figure 30 - Comparison of Initial and Final Mesh Using Nonlinear Static Analysis

From this comparison it can be seen that the results are very similar between the two meshes. The response during the elastic portion of the analysis are almost identical. Continuing through the analyses some differences do appear, but they are minimal, with the maximum load factor difference experienced being 0.00291. The final mesh chosen computationally saves time because of the decrease of elements, and the results from the pushover analysis are more conservative compared to the initial mesh. For these reasons this mesh was chosen to continue the analysis of the Mallorca Cathedral.

4.2 Equivalent Two-Dimensional Model

An equivalent two-dimensional model was used throughout this research to reduce computational time. To determine the equivalency, the two-dimensional model developed by (Roca, Cervera, Pela, Clemente, & Chiumenti, 2013) was considered. This model consisted of a typical bay of the Mallorca Cathedral, as in this study. In the study by (Roca, Cervera, Pela, Clemente, & Chiumenti, 2013) a nonlinear structural analysis was considered; therefore, the same analysis was performed on the equivalent two-dimensional model to allow for comparison of the models.

For clarity the 'Reference Model (Roca et al, 2013)' is defined as the capacity curve obtained from (Roca, Cervera, Pela, Clemente, & Chiumenti, 2013) through pushover analysis. While the 'Equivalent Model with Parameters from Roca et al. 2013' refers to the model obtained using the mechanical properties from (Roca, Cervera, Pela, Clemente, & Chiumenti, 2013).

Figure 31 displays the resulting capacity curves.

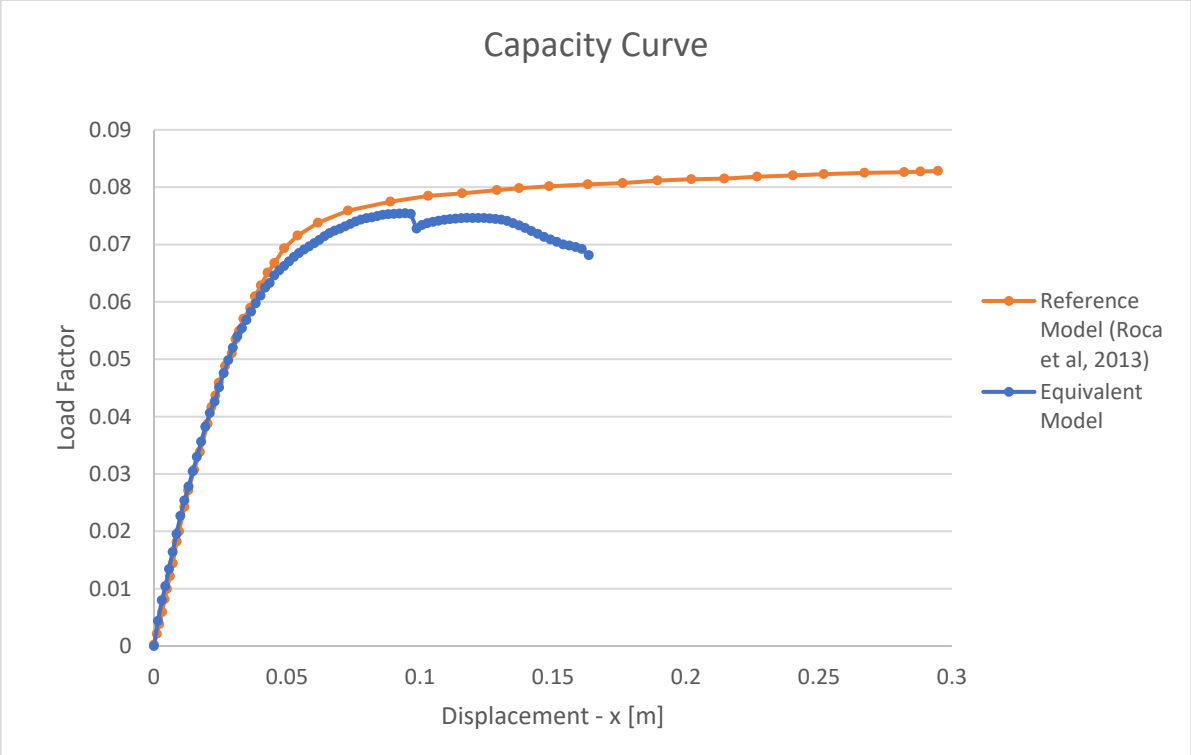

Figure 31 – Comparison of Capacity Curve of Equivalent Model to Reference Model (Roca, Cervera, Pela, Clemente, & Chiumenti, 2013)

As seen in Figure 31, the stiffness of the two models is the same. This was the main objective of comparison through this analysis. The difference in the nonlinear response can be attributed to the difference in the models. The equivalent model used an arc-length technique to obtain the post-peak response, while (Roca, Cervera, Pela, Clemente, & Chiumenti, 2013) the loading was increased monotonically.

The following section further details the nonlinear static analysis and the damage occurred during the analysis to the equivalent two-dimensional model.

4.3 Nonlinear Static Analysis and Damage Pattern

Further evaluation of the nonlinear static analysis and the resulting damage pattern of the equivalent two-dimensional model was completed for further understanding of the behaviour of the structure. This behaviour allows for the crack orientation to rotate with the axis of the principal strain. To simulate the nonlinear effects both physical and geometrical nonlinearity was considered, for the geometric nonlinearity Total Lagrange was considered. In nonlinear static analysis there are two phases in the loading of the structure. First, the self-weight of the structure is applied incrementally. Secondly, an incremental load proportional to mass was applied horizontally until the collapse of the structure. During the horizontal loading of the structure an arc length method was applied to ensure the post peak behaviour could be captured. After a preliminary analysis of the iteration method the Regular Newton

Raphson Method was determined to obtain the most stable results. As for the convergence criteria both force and displacement criteria were considered, with a tolerance of 1%. The capacity curve obtained from the pushover analysis can be seen in the following figure, Figure 32.

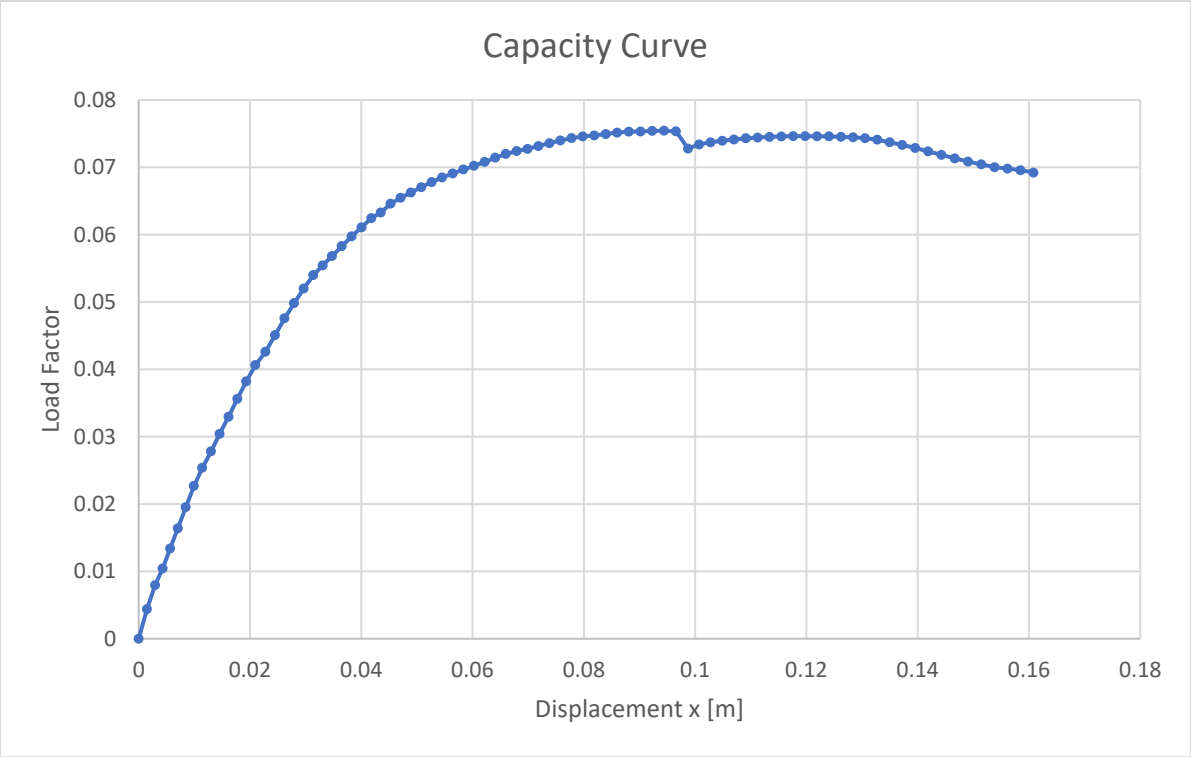

Figure 32 - Capacity Curve - Equivalent Model

The evolution of damage can also be analyzed from this investigation through the development of the cracks in the structure. The evolution of the damage can be seen in the following figures, Figure 33, Figure 34, Figure 35, and Figure 36, starting with the first sign of damage, the damage experienced when the full self-weight is applied, at the maximum loading, and at failure. As seen in Figure 33 the first damage was experienced at 0.2 self-weight, in the openings in the buttresses at the key and base.

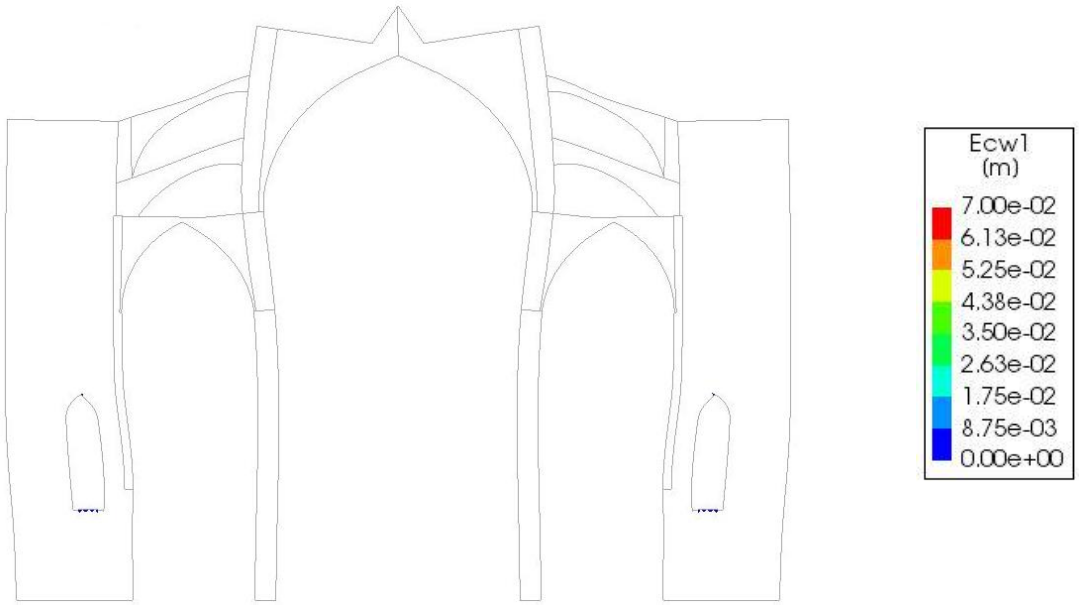

Figure 33 - First Developed Crack: Buttress Openings - 0.2 Self-Weight – Equivalent Model

Furthermore, continuing the analysis, at the full self-weight, the damage in Figure 34 was obtained. The damage is concentrated at the openings – in the buttress, the center of the vaults, as well as the connection between the flying arches and the clerestory.

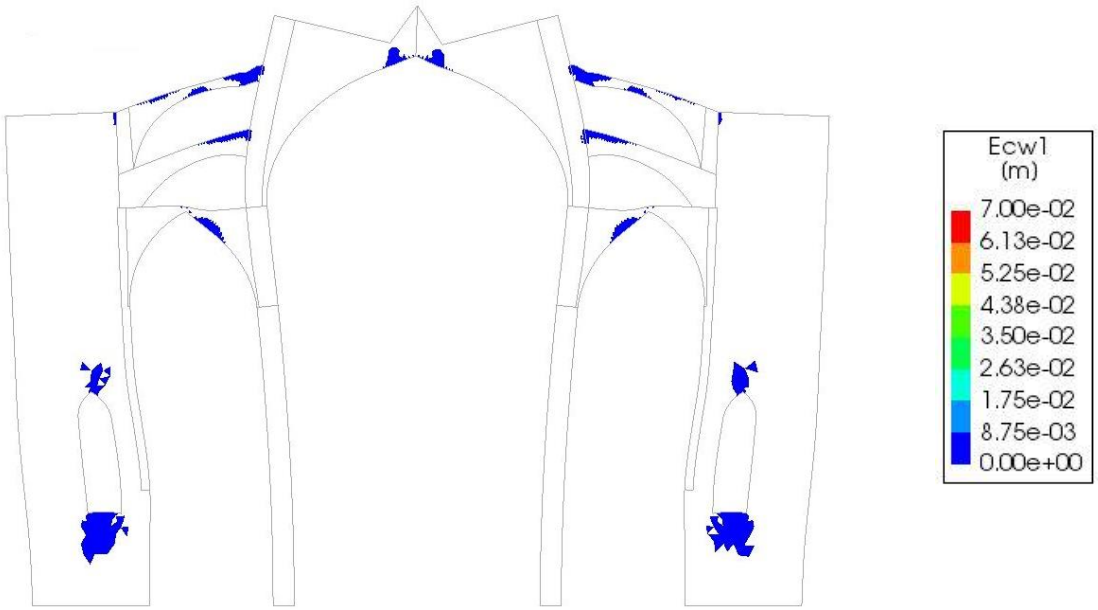

Figure 34 – Crack Width in First Principle Direction Under Full Gravity Load – Equivalent Model

The maximum load during the pushover analysis was a load factor of 0.074703, the cracks occurred at this instant are shown in the figure below, Figure 35. The cracking concentrated at the openings – in the buttress, flying arches, and vaults. Cracks also started to form in the base of the right column.

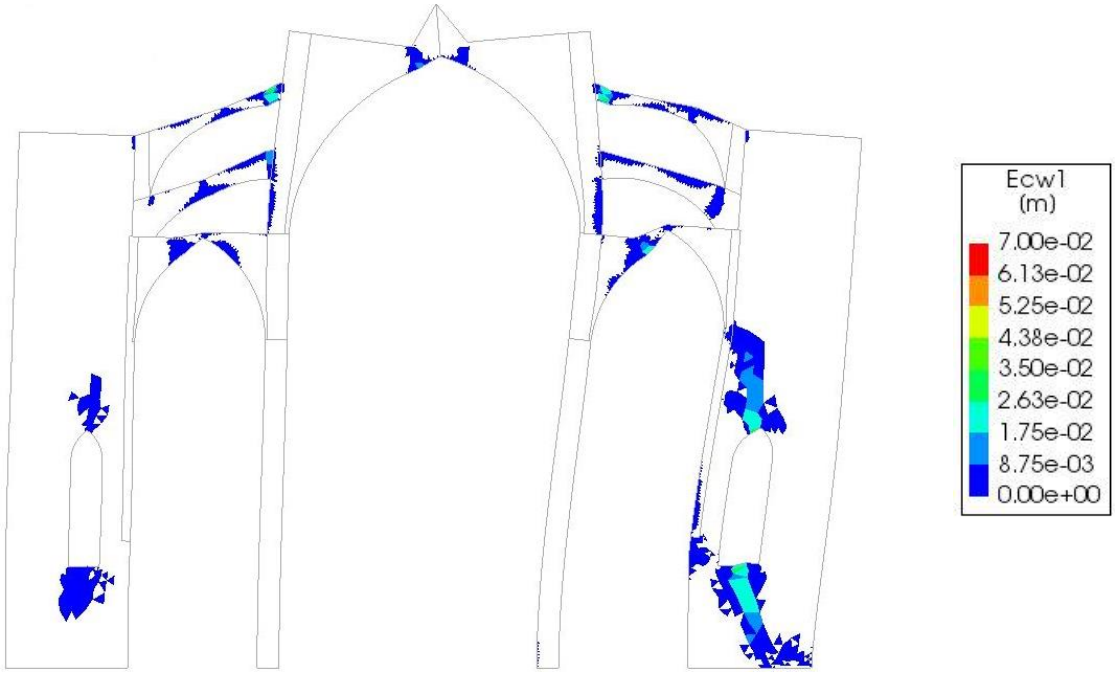

Figure 35 - Crack Width in First Principle Direction Under Maximum Loading Conditions of Pushover Analysis – Equivalent Model

Continuing the analysis results in the following damage, a maximum displacement of 0.19m at the top right flying arch and the top of the right buttress. In this instance there is a lot of damage in the right buttress from compression. As well as damage in the center of the vaults and in the flying arches. The largest cracks located at the connection between the top left flying arch and the clerestory.

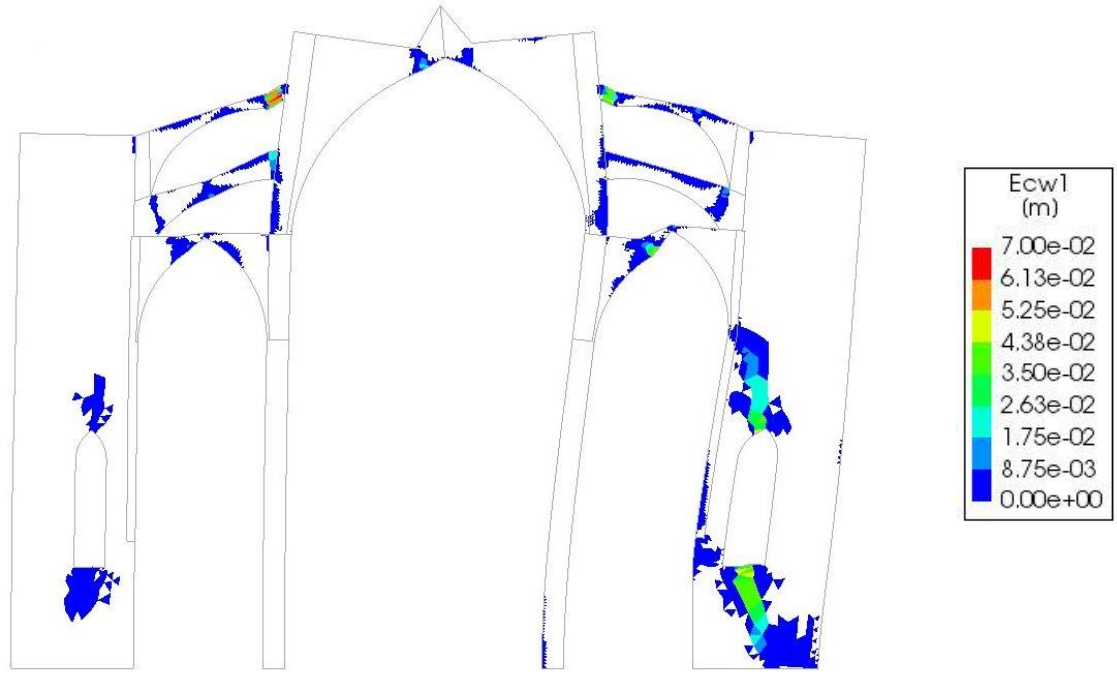

Figure 36 - Crack Width in First Principle Direction Under Maximum Displacement of Pushover Analysis – Equivalent Model

These results can be compared to the previous study by (Roca, Cervera, Pela, Clemente, & Chiumenti, 2013), where a similar pushover analysis was conducted. The resulting cracking and deformed shape is shown in the figure below. Comparing the two, there are some similarities in the response to the seismic force. Cracking began developing similar to the developed damage seen in Figure 37, as well as the deformed shape. Some of the differences in the equivalent two-dimensional model when comparing it to the model prepared by (Roca, Cervera, Pela, Clemente, & Chiumenti, 2013) include damage on the bottom of the left column and left bottom corner of the left buttress. While most of the damage in the equivalent model is less than the model developed by (Roca, Cervera, Pela, Clemente, & Chiumenti, 2013), the damage developed on the right side of the main vault is larger in the equivalent model.

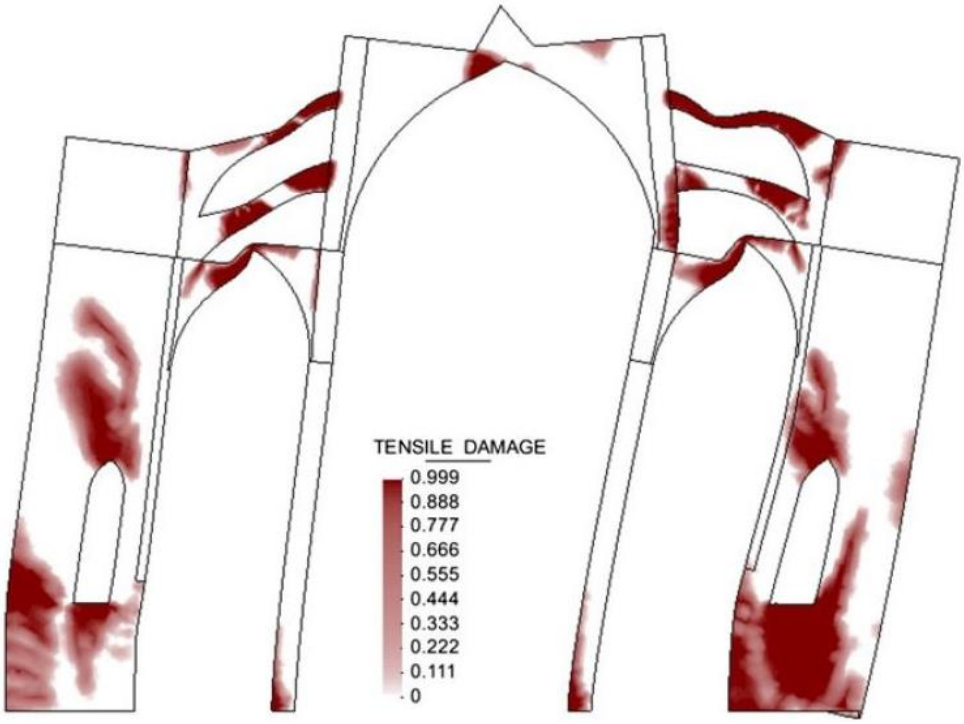

Figure 37 – Deformed Shape and Tensile Damage (Roca, Cervera, Pela, Clemente, & Chiumenti, 2013)

5. UNCERTAINTY EVALUATION

Even though in Section 4 deterministic values were used there are multiple reasons for the values obtained from previous studies to deviate from reality. First there are aleatoric uncertainties due to the natural variability or randomness of the material. Secondly, there are epistemic uncertainties as the information obtained could be imprecise. Also, it is not definite that numerical models treat materials properties the same as the real-world (Petromichelakis, Saloustros, & Pela, 2014). The uncertainty of the mechanical properties was considered with the randomization of the tensile strength, compressive strength, and Young's modulus using a Monte Carlo simulation. The following sections describe the process which was used to obtain the material properties that were used in the 200 nonlinear static analyses.

5.1 Identified Random Variables

The variables that were simulated as random variables during the Monte Carlo simulation were the tensile strength, compressive strength, and Young's modulus. Three material groups were considered for this simulation: first the columns and flying arches, secondly the vaults, and finally buttresses and clerestories. These groups were determined based on the similarity of materials. In the study by (Roca, Cervera, Pela, Clemente, & Chiumenti, 2013) the material groups were very similar, but the vault, buttresses, and clerestories were grouped together. The vaults were separated from the buttresses and clerestories because the buttress was found to be made of three wythe masonry (Roca, et al., 2008).

5.2 Monte Carlo Simulation

A Monte Carlo simulation is a mathematical process used to generate sets of numbers that resemble samples from a larger population. This process is completed with the following procedure. A computer algorithm is used to generate a pseudo-sample from a pseudo population, this sample is generated creating a number of trials, where a relative frequency distribution is constructed. The Monte Carlo simulation can generate three different types of data including constants, deterministic variables, and random variables (Mooney, 1997).

For the Monte Carlo Simulation the vaults were considered as the reference material. The compressive strength, tensile strength, and Young's Modulus of the vaults were considered as random materials. These properties of the other materials; columns and flying arches, and buttresses and clerestories; were considered using percentage coefficients to relate to the reference material. In the following table the variables used to represent these properties are presented.

Table 5 – Variables Used in Monte Carlo Simulation

Compressive Strength	f_c
Tensile Strength	f_t
Young's Modulus	E
Percentage Coefficient – Column and Flying Arch	C_{coeff}
Percentage Coefficient – Buttress and Clerestory	B_{coeff}

The values were determined according to table C8A.2.1 in Appendix C8A of the Italian Recommendations (IMIT, 2009). From a literature review, and comparison to the values used in (Roca, Cervera, Pela, Clemente, & Chiumenti, 2013) the corresponding category for each material group was determined. Firstly, the columns and flying arches were determined to be of good quality stone, well-cut, and has good interlocking (Perez-Gracia, Caselles, Martinez, & Osorio, 2013). This resulted choosing the fifth category "Muratura a blocchi lapidei squadrati" (dressed rectangular stone masonry) (IMIT, 2009). This category also corresponds to the compressive strength used in (Roca, Cervera, Pela, Clemente, & Chiumenti, 2013) 8MPa. The same category was also used for the vaults because the same masonry typology was determined in previous visual inspection. As for the buttress and clerestory the second category "Muratura a conci sbozzati, con paramento di limitato spessore e nucleo interno" (uncut stone with facing walls of limited thickness and infill core) (IMIT, 2009) was used. This is due to the fact that in a previous study, using ground-penetrating radar and a coring sample, the buttresses were concluded to be three wythe with external leaves of 35cm and an inner core of poorer quality and easily workable limestone block masonry (Roca, et al., 2008). Table C8A.2.2. in appendix C8A of the Italian Code was also considered to determine the correction coefficients for the corresponding ranges for the material properties. In this case, a correction coefficient was only considered for the material of the columns and flying arches. A correction coefficient of 1.2 was determined to be suitable due to the squared blocks and interlocking as previously mentioned (IMIT, 2009). This results in the following minimum and maximum the compressive strengths shown in Table 6.

Table 6 - Compressive Strength Minimum and Maximum Values Used in Monte Carlo Simulation (IMIT, 2009)

Material	f_c [N/mm^2]	
	Min	Max
Vault	6	8
Column & Flying Arch	7.2	9.6
Buttress & Clerestory	2	3

In terms of Young's Modulus and tensile strength, a function of compressive strength was applied. Considering table C8A.2.1 from the Italian Code, again, the range of Young's Modulus was determined to be $500f_c$ – $700f_c$, while the tensile strength was determined to be $2\%f_c$ – $5\%f_c$. This results in the material property ranges in Table 7 (IMIT, 2009).

Table 7 – Minimum, Maximum, and Mean Material Properties Used in Monte Carlo Simulation (IMIT, 2009)

Material	f_c [N/mm^2]			f_t [N/mm^2]			E [N/mm^2]		
	Min	Max	Mean	Min	Max	Mean	Min	Max	Mean
Vault	6	8	7	0.12	0.4	0.26	3000	5600	4300
Column & Flying Arch	7.2	9.6	8.4	0.144	0.48	0.312	3600	6720	5160
Buttress & Clerestory	2	3	2.5	0.04	0.15	0.095	1000	2100	1550

The material of the vaults was considered to be the reference material in this simulation. The other materials were then determined as percentages of the reference material. These coefficients are presented in Table 8.

Table 8 – Dependent Materials' Percentage Coefficients

Material	Percentage Coefficients	
Column and Flying Arch	C_{coeff}	1.1-1.3
Buttress and Clerestory	B_{coeff}	0.33-0.5

The density was not included in the random variables because it was used to calibrate the two-dimensional model to the three-dimensional model. As for the fracture energy both the compressive and tensile fracture energy was calculated based on the compressive strength. The tensile fracture energy is calculated according to Equation (2) using the assumption according to (CEB-FIP, 1993) that the maximum aggregate size was 8mm resulting in f_{cmo} equalling 10 N/mm^2 (Lourenco, 2009).

$$G_f^t = 0.025\left(\frac{f_{cm}}{f_{cmo}}\right)^{0.7} \quad (2)$$

While the compressive fracture energy was calculated using the ductility index, as seen in Equation (3). As in (Lourenco, 2009) the ductility index is assumed to be 1.6mm.

$$d = \frac{G_f^c}{f_c} \quad (3)$$

When simulating the uncertainties, a log-normal distribution was determined for the mechanical properties – tensile strength, compressive strength, and Young's Modulus (CNR-DT, 2013). While the percentage coefficients were a uniform probability distribution. To determine the logarithmic parameters Table 3.1 of (CNR-DT, 2013) was used. The mean of the existing ranges was calculated, and Table 3.1 was used to determine the logarithmic standard deviation. Once the logarithmic mean was determined using the following formula (CNR-DT, 2013).

$$\mu_{ln} = ln\mu - \frac{1}{2}\sigma_{ln}^2 \quad 4$$

This resulted in the following logarithmic parameters, Table 9.

Table 9 - Logarithmic Mean and Deviation of Random Variables for Reference Material

Variable	μ_{ln}	σ_{ln}
Compressive Strength	1.94	0.05
Tensile Strength	-1.37	0.22
Young's Modulus	8.36	0.12

The data obtained from the Monte Carlo simulation is displayed in the following graphs, showing the frequency of each of the random variables; compressive strength, tensile strength, ad Young's Modulus.

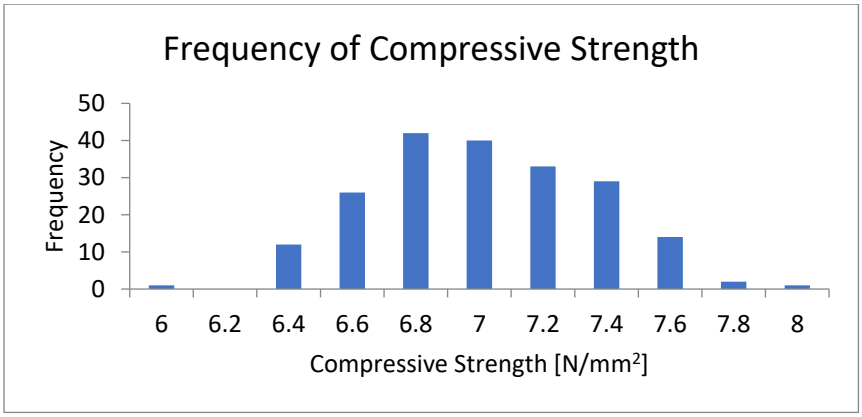

Figure 38 - Frequency of Compressive Strength from Monte Carlo Simulation

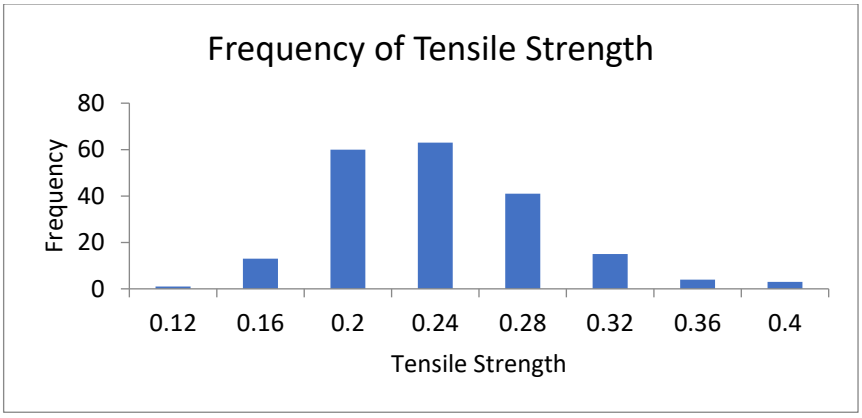

Figure 39 - Frequency of Tensile Strength from Monte Carlo Simulation

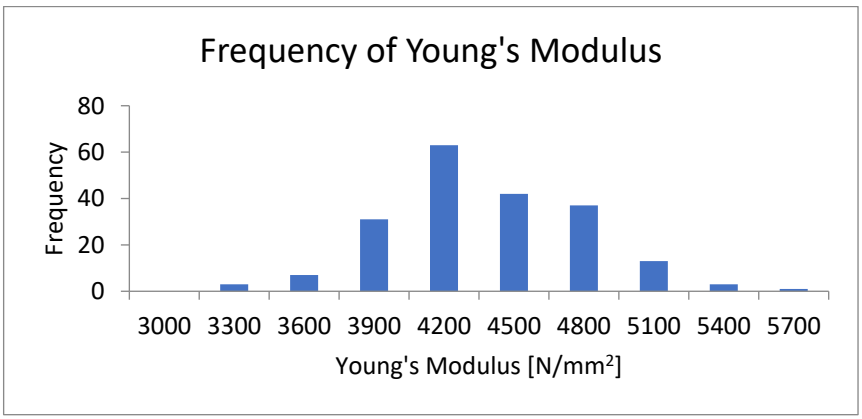

Figure 40 - Frequency of Young's Modulus from Monte Carlo Simulation

5.3 Reference Model

A reference model was prepared using the mean values of the minimum and maximum values from Table 7. The compressive strength, tensile strength, and Young's Modulus can be seen in Table 10.

Table 10 - Material Properties of Reference Model

Material	f_c [N/mm^2]	f_t [N/mm^2]	E [N/mm^2]
Vault	7	0.26	4300
Column & Flying Arch	8.4	0.312	5160
Buttress & Clerestory	2.5	0.095	1550

The tensile fracture energy and compressive fracture energy were calculated using the mean compressive strength of each material using equation (2) and (3). The Poisson's ratio was assumed to be the same as the values in Table 3.

A nonlinear static analysis was completed to allow for the comparison of the reference model and the equivalent model with parameters from (Roca, Cervera, Pela, Clemente, & Chiumenti, 2013), resulting in the following capacity curve, Figure 41.

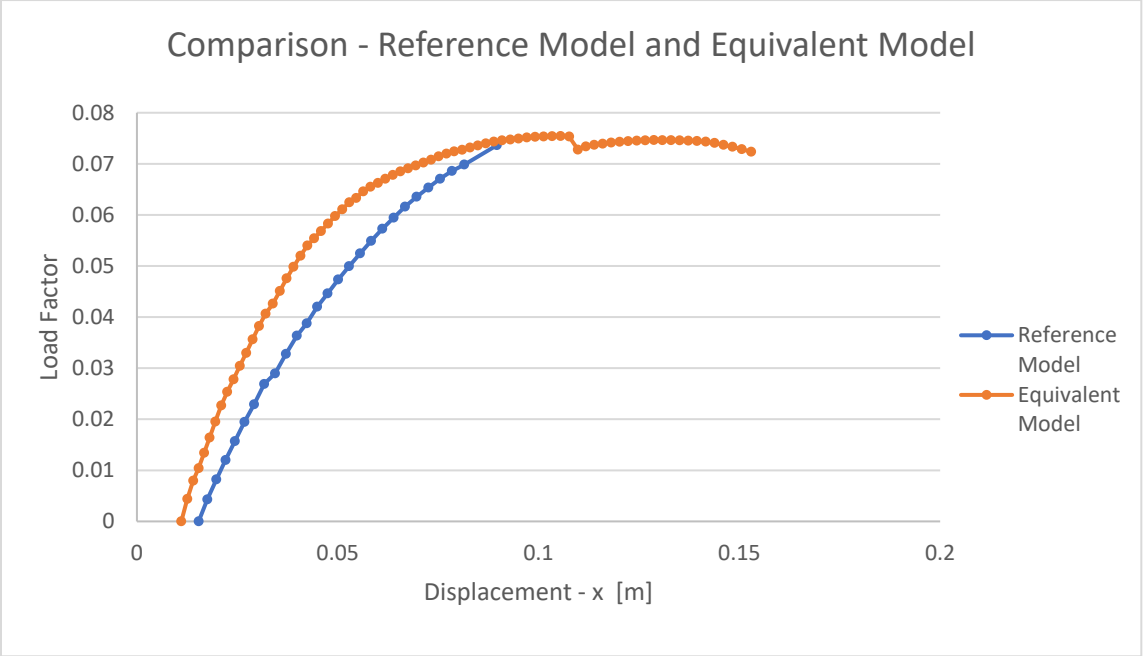

Figure 41 – Comparison of Reference Model and Equivalent Model

The damage evolution was also examined for the reference model. In this model the damage was first experienced at 0.15 self-weight at the key and base of the opening in the buttresses. The evolution can be seen in the following figures of the crack width at the first damage, full self-weight, maximum load, and maximum displacement.

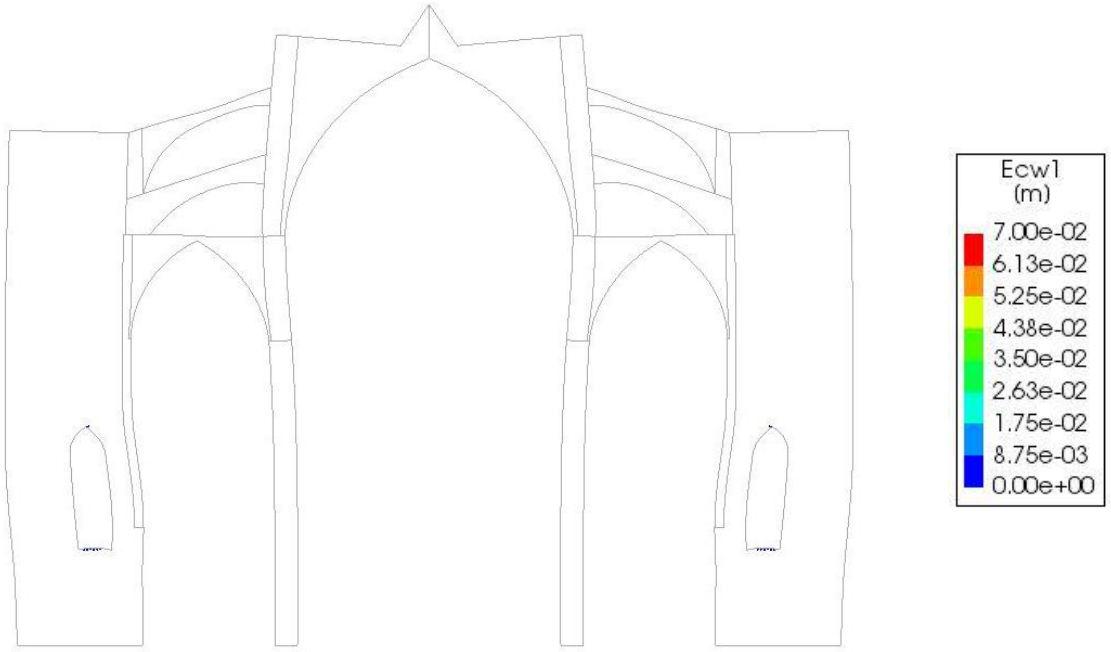

Figure 42 – Contour of Crack Widths in the Principle Direction - First Developed Crack: Buttress Opening - 0.15 Self-Weight - Reference Model

Continuing the analysis to the application of the entire self-weight results in the following damage pattern. In comparison to the original model, there is an increase in the number of cracks, many are in the same, or a similar location. Additional cracks are located at the connection between the flying arches.

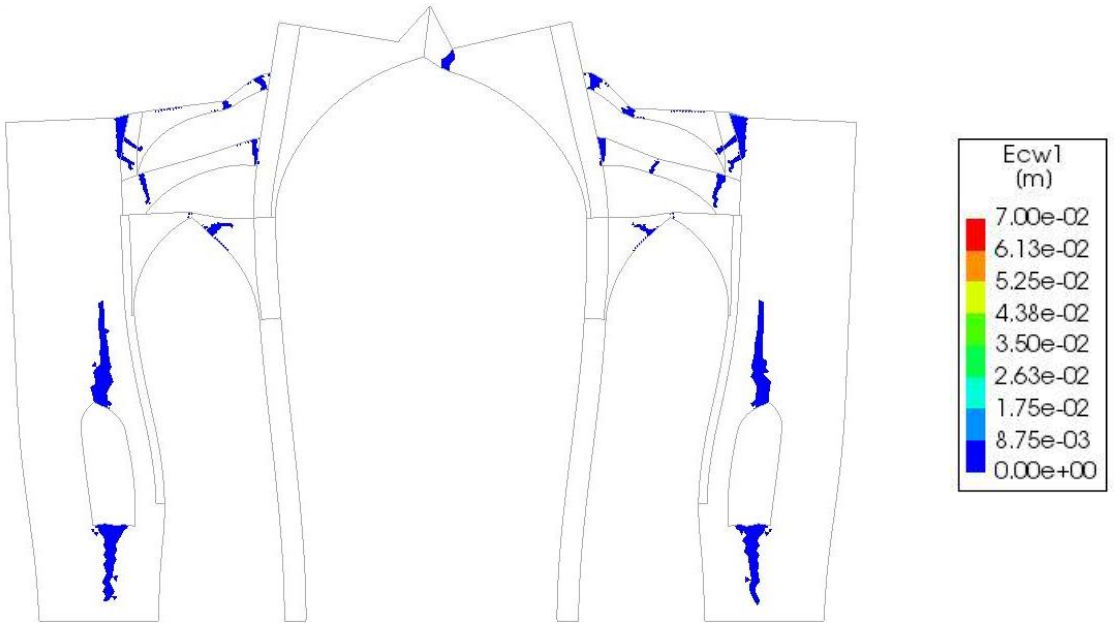

Figure 43 – Contour of Crack Widths in First Principle Direction Under Gravity Load - Reference Model

Through the seismic loading of the reference model, the first new crack developed on the middle of the lower left flying arch, increasing throughout the loading process. The next crack developed in the left

upper portion of the main vault. Followed by cracking near the connection between the left lateral vault and clearstory, the right buttress and finally, in the right buttress near the lateral clerestory and in the lateral clerestory.

The maximum load occurred through this analysis was a load factor of 0.073636. The damage pattern is shown below, an increase of the existing cracks, as well as cracking in the center of the flying arches, and the connection between the flying arches and the clerestory. The post peak behaviour of the reference model was not obtained. Therefore, the maximum displacement was also as shown in the deformed shape. The maximum displacement was 0.11m at the top of the right buttress and the left half of the right lateral vault.

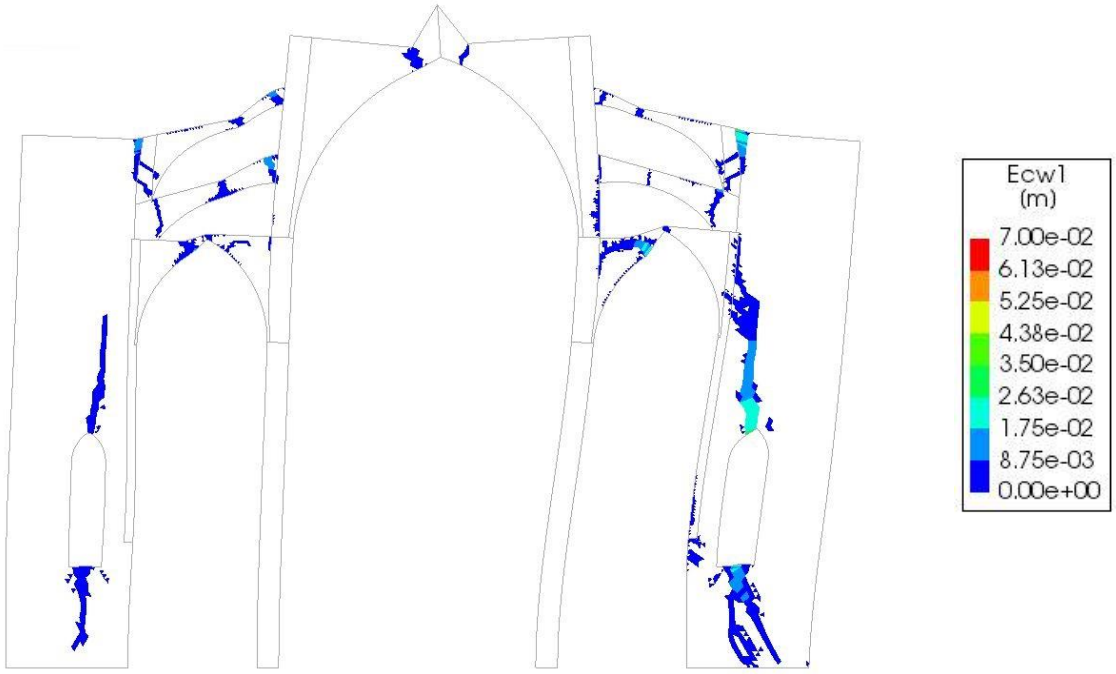

Figure 44 – Contour Crack Widths in Frist Principle Direction at Maximum Load of Pushover Analysis - Reference Model

6. PROBABILISTIC SEISMIC ASSESSMENT

The variables generated in the previous section were used to conduct a probabilistic seismic assessment through the case study of the Mallorca Cathedral.

6.1 Nonlinear Static Analyses – Capacity Curves

This assessment was conducted by developing pushover analyses for all 200 mechanical material property combinations that were generated during the Monte Carlo simulation. The capacity curves are shown in Figure 45 in terms of spectral acceleration and displacement at the top of the right column.

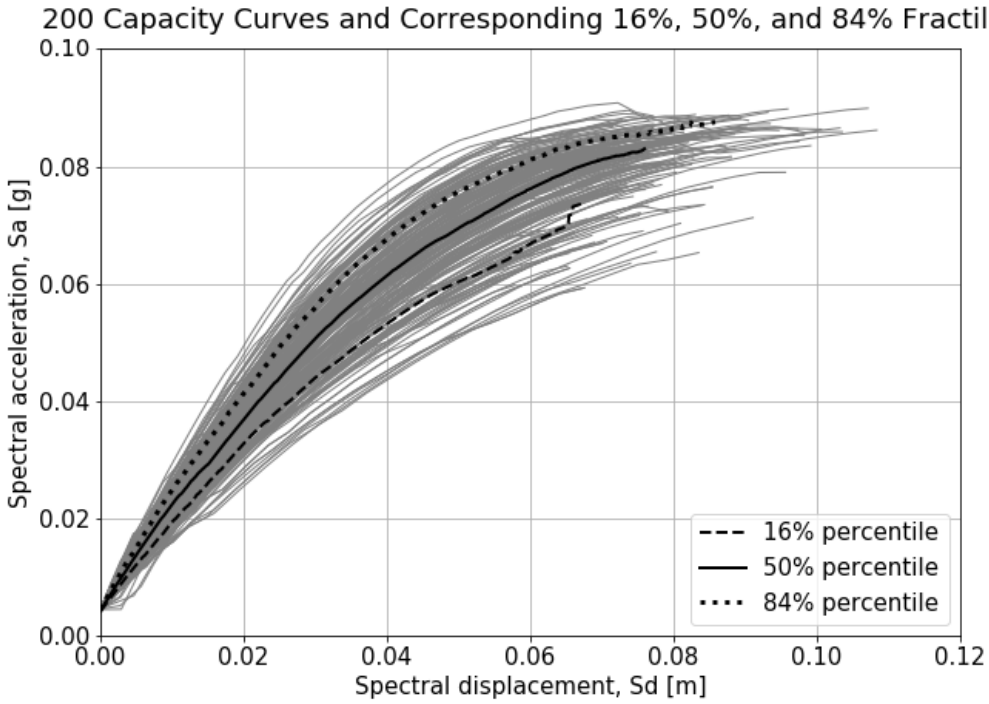

Figure 45 – 200 Capacity Curves from 200 Pushover Analyses Including 16th, 50th, and 84th Percentile

In the initial loading of the pushover analyses there is generally a smaller difference in the behaviour. While in the final capacity a 39.88 % difference was found between the highest capacity, 0.08884 g, and the lowest capacity, 0.0593 g.

A comparison of the reference, mean, and median was completed, as shown in Figure 46. The mean and median capacity curves, as well as the capacity curve obtained from the reference material properties from Table 10.

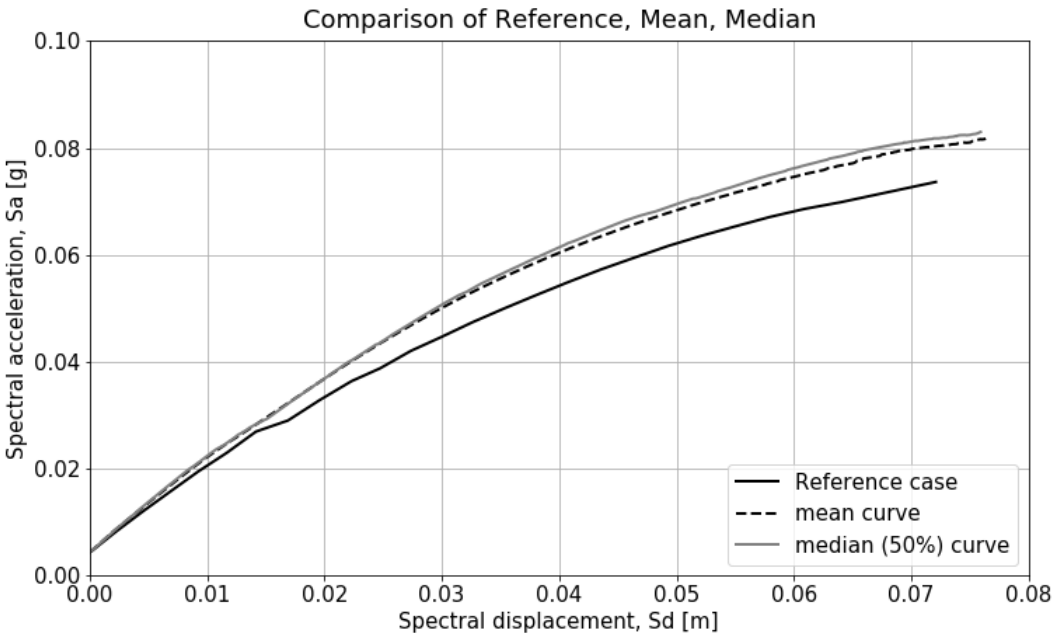

Figure 46 – Reference, Mean, and Median Curve of Uncertainty Analysis

All three curves are similar in the beginning of the loading. The reference curve becomes more conservative while the mean and median curve continue to have a similar response until later in the loading where the mean curve becomes more conservative. The difference seen in the mean and reference case suggests an unsymmetrical influence of one or more parameters.

An investigation into the post-peak behaviour was completed to validate the obtained results. Various analyses have been performed considering: (a) smaller loading increments, (b) different reference node for the arc length strategy, (c) continuation of the analysis even if the convergence criteria are not satisfied, and (d) increase of the fracture energy. All of the obtained capacity curves are shown in Figure 47. None of the obtained capacity curves showed a large increase in the obtained post-peak behaviour.

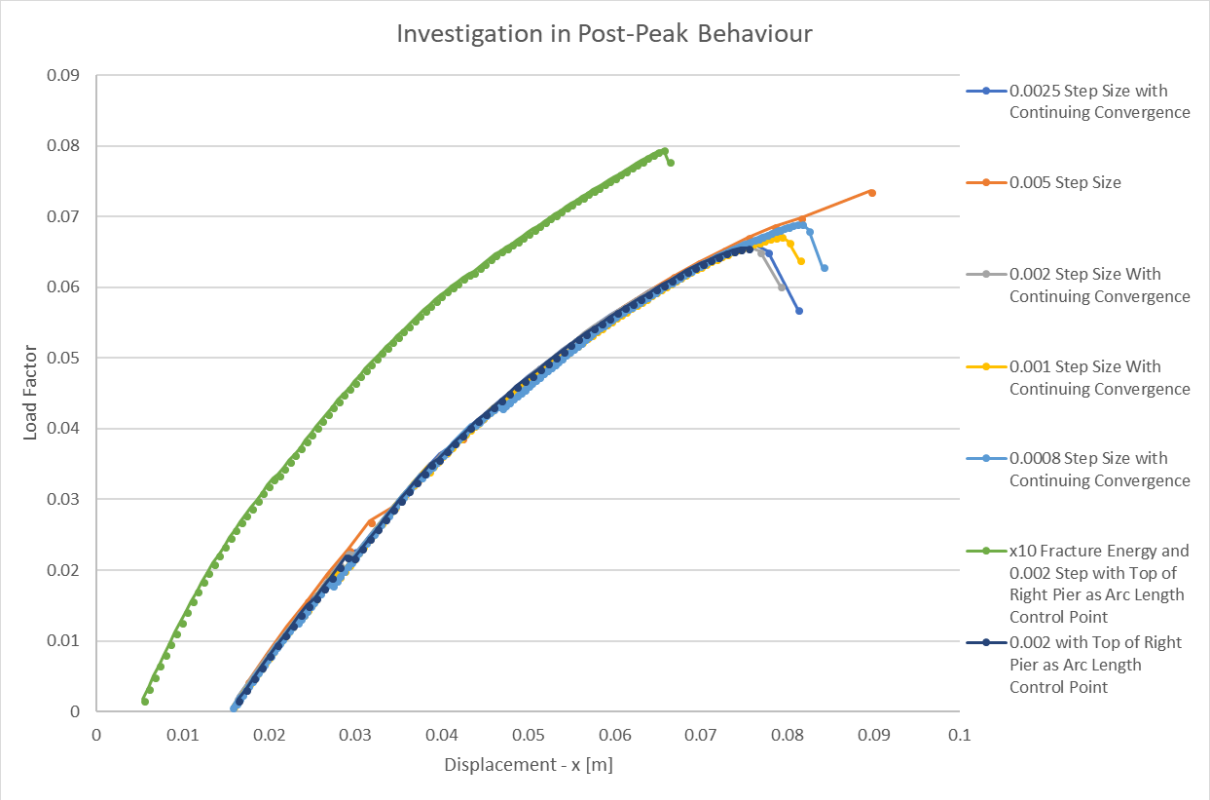

Figure 47 – Investigation in Post-Peak Behaviour – Decrease in Load Step Size, Continuing Convergence, Increase in Fracture Energy, and Change of Arc Length Control Point to Top of the Right Pier

In order to identify if the end of the analysis coincides with the evolution of a local or global collapse mechanism some of the models were analysed a second time considering the continuation of the analysis in the case that the convergence criteria were not met. Models A022, A029, and A151 are presented. Model A022 had the highest capacity, while A029 had a median capacity, and A151 had the lowest capacity These models have the mechanical properties as presented in Table 11.

Table 11 – Mechanical Properties of Representative Models of Uncertainty Analysis

Model Number:	A022	A029	A151
Vaults			
f_c [N/mm^2]	7.260	6.780	6.560
f_t [N/mm^2]	0.237	0.229	0.169
E [N/mm^2]	4750	4870	3560
Columns and Flying Arches			
f_c [N/mm^2]	7.980	7.790	8.530

f_t [N/mm^2]	0.260	0.263	0.220
E [N/mm^2]	5230	5600	1240
Buttress and Clerestory			
f_c [N/mm^2]	3.630	2.710	2.300
f_t [N/mm^2]	0.118	0.0915	0.0593
E [N/mm^2]	2380	1950	1240

The last loading step before the analyses diverged are shown below in Figure 48, Figure 49, and Figure 50, to understand the collapse of each model.

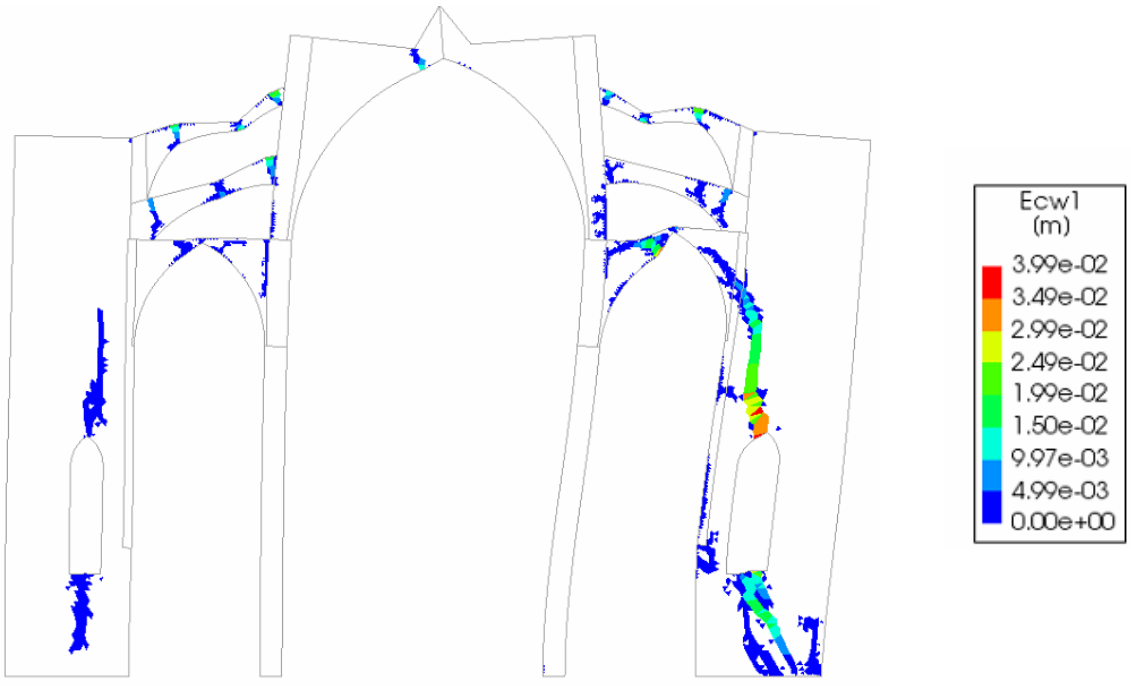

Figure 48 - Collapse of Model A022: Model with Maximum Capacity

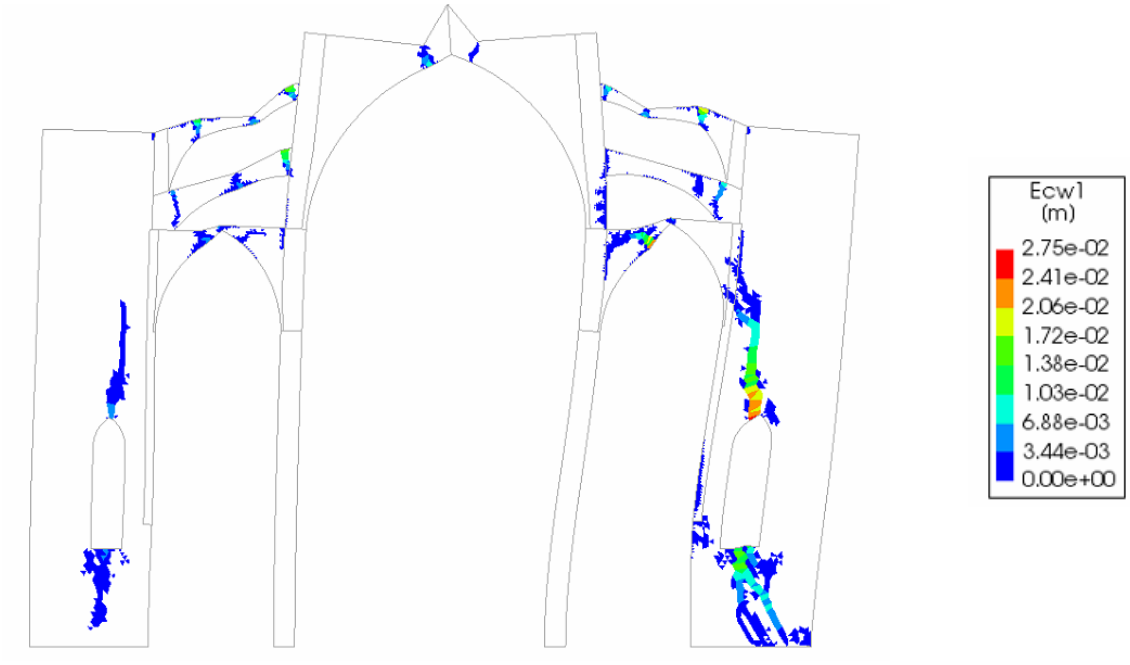

Figure 49 – Collapse of Model A029: Model with Median Capacity

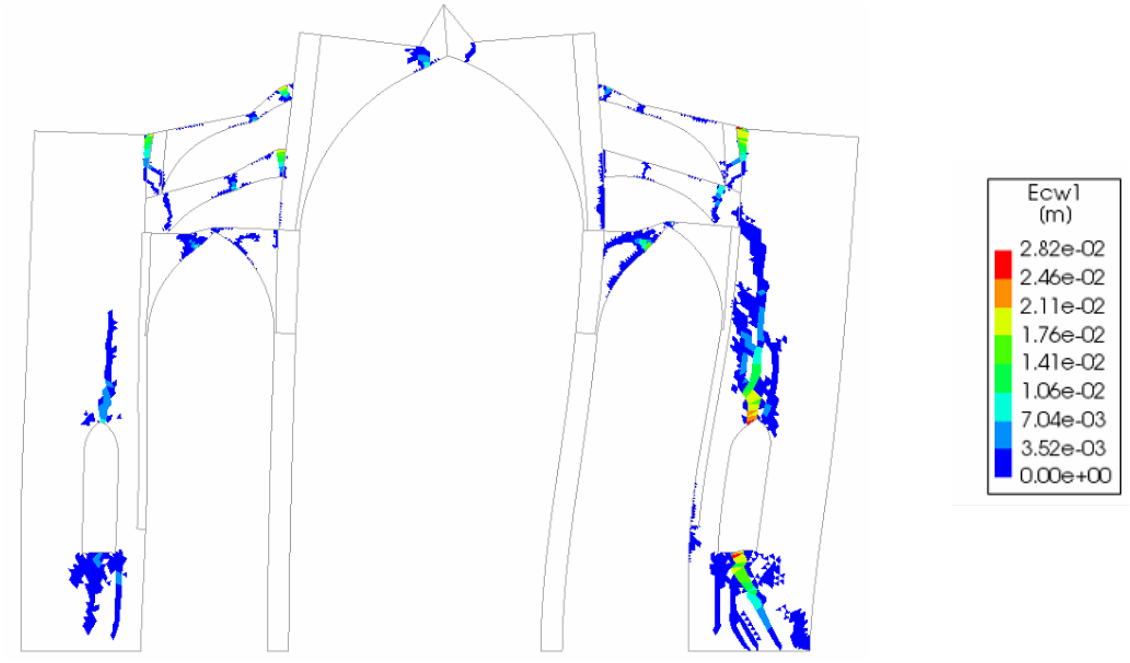

Figure 50 – Collapse of Model A151: Model with Minimum Capacity

Models A022 and A029 show a local collapse of the top right flying arch and a possible shear failure of the right buttress. While, model A151 shows a possible shear failure of the buttress.

Therefore, from these analyses it was determined that a brittle local collapse mechanism was experienced, therefore, validating the lack of post-peak behaviour in Figure 45.

6.2 Application of the Mechanical Approach

For each of the 200 capacity curves obtained in the last section the mechanical approach was applied. The mechanical approach is a capacity spectrum-based method. The performance of the structure is based on the intersection of the capacity curve and earthquake demand curve (Lagomarsino & Giovinazzi, 2006).

There are three main steps of this approach; idealization of the capacity curves, definition of the damage grades, and the definition of the fragility curves. The methodology and results of the mechanical approach are discussed in the following subsections.

6.2.1 Idealization of Capacity Curves

Using the obtained capacity curved in the last section the curves were idealized to an elasto-plastic bilinear capacity curve, using the following methodology.

The structure is modelled as a single degree of freedom system, neglecting hardening and softening of the structure, as shown in Figure 51.

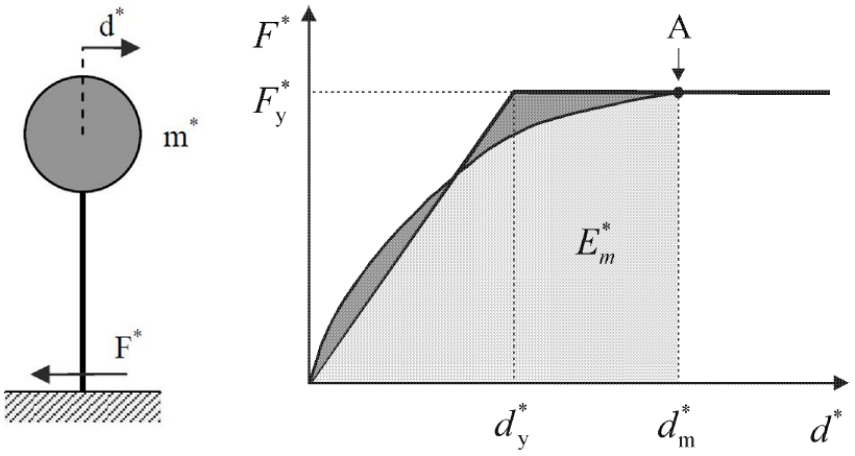

Figure 51 – Graphical Representation of N2 Method – Equivalent Single Degree of Freedom System (left) and Bilinear Capacity Curve (right) (IMIT, 2009)

The base shear (F_b) and displacement at the control node (d_b) are transformed into force (F*) and displacement (d*) with the transformation factor (Γ) using Equation 5 and Equation 6 (European Committee for Standardization, 2004).

$$F^* = \frac{F_b}{\Gamma} \qquad 5$$

$$d^* = \frac{d_b}{\Gamma} \quad 6$$

The transformation factor (Γ) or the modal participation factor, defined for the reference model, was calculated using Equation 7 (European Committee for Standardization, 2004), in terms of the mass of each node (m_j) and the corresponding modal displacement (φ_j).

$$\Gamma = \frac{\sum \varphi_j m_j}{\sum \varphi_j^2 m_j} \quad 7$$

Next, a simplification of the system's behaviour was completed to obtain a bilinear curve. This must result in the area under the original curve and the bilinear curve from zero to d_m^* must be equal. For this to be ensured the yield displacement is calculated using Equation 8 (European Committee for Standardization, 2004).

$$d_y^* = 2\left(d_m^* - \frac{E_m^*}{F_y^*}\right) \quad 8$$

Where:

E_m^* is the actual deformation energy at the formation of the plastic mechanism.

F_y^* is the base shear force at the formation of the plastic mechanism.

d_m^* is the displacement at the formation of the plastic mechanism.

The period of the idealized equivalent single degree of freedom system (T*) was determined using Equation 9 (European Committee for Standardization, 2004), with yield strength (F_y*), displacement (d_y*), and equivalent mass (m*).

$$T^* = 2\pi\sqrt{\frac{m^* d_y^*}{F_y^*}} \quad 9$$

While the equivalent mass (m*) was calculated using Equation 10 (European Committee for Standardization, 2004).

$$m^* = \sum \varphi m \quad 10$$

An equivalent bilinear capacity curve was obtained for each of the 200 analyses. A bilinear curve and single degree of freedom capacity curve can be seen in Figure 52.

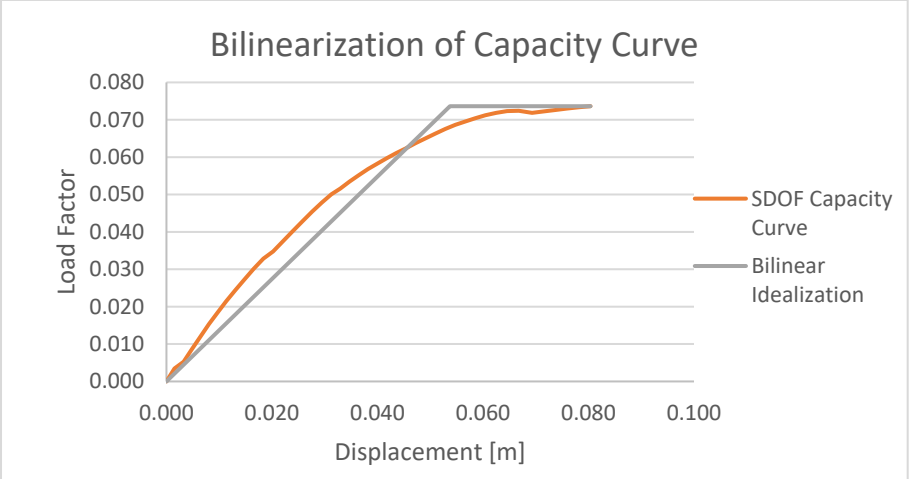

Figure 52 – Bilinearization of Capacity Curve

6.2.2 Definition of Damage Grades

Next, the damage grades were defined as a function of yield displacement (d_y) and ultimate displacement (d_u) of the bilinear capacity curve, similar to the method suggested in (Lagomarsino & Giovinazzi, 2006). Due to a short plastic portion of the bilinear capacity curve the second damage grade from (Lagomarsino & Giovinazzi, 2006) was not considered. The limits are presented in Table 12, below.

Table 12 - Damage Grades (Lagomarsino & Giovinazzi, 2006)

$S_{d,1}$	$0.7d_y$
$S_{d,2}$	$0.5(d_y + d_u)$
$S_{d,3}$	d_u

These damage grades are represented on the graph in Figure 53.

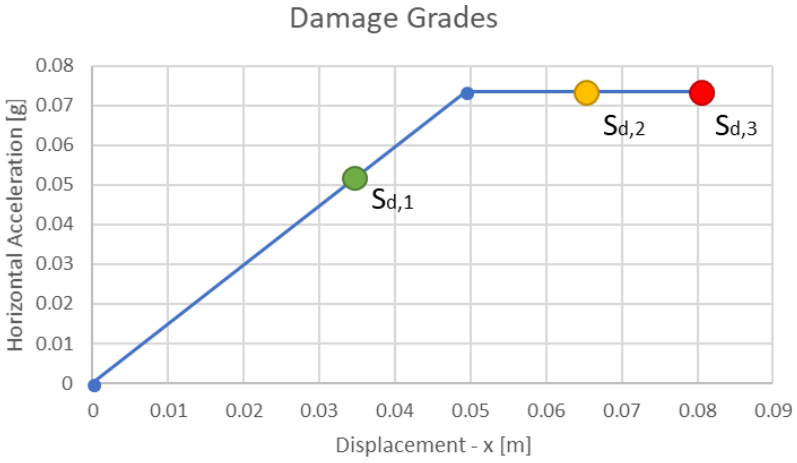

Figure 53 – Damage Grades on Bilinear Idealized Capacity Curve

6.2.3 Definition of Fragility Curves

Finally, the fragility curves were derived. Frist, the elastic response spectrum for the site was derived according to Eurocode 8 (European Committee for Standardization, 2004). The soil type of the Mallorca Cathedral was determined to be soil type “B” according (Elyamani, 2015). The spectral parameters of soil type B are outlined in Table 13.

Table 13 – Values for Elastic Response Spectra from Eurocode 6

Ground Type	S	T_B(s)	T_C(s)	T_D(s)
B	1.2	0.15	0.5	2

The displacement response spectrum was determined using Equation 10 (European Committee for Standardization, 2004).

$$S_{De}(T) = S_e(T)\left[\frac{T}{2\pi}\right]^2 \quad 10$$

The Spectrum was built according to Equation 11, Equation 12, and Equation 13 (European Committee for Standardization, 2004).

$$d^* = S_{De}(T^*)\ for\ T^* \geq T_C \quad 11$$

$$d^* = S_{De}(T^*)\ for\ T^* \leq T_C\ and\ \frac{F_y^*}{m^*} \geq S_e(T^*) \quad 12$$

$$d^* = \frac{S_{De}(T^*)}{q_u}\left(1 + (q_u - 1)\frac{T_C}{T^*} \geq S_{De}(T^*)\right)\ for\ T^* \leq T_C\ and\ \frac{F_y^*}{m^*} \geq S_e(T^*) \quad 13$$

Once the limit states were derived for the structure, the fragility curves were derived with the following function, Equation 14 (ATC-58, 2009), considering the lognormal cumulative density.

$$P[LSi|Z] = \Phi\left(\frac{ln\left(\frac{Z}{\theta_i}\right)}{\beta_i}\right) \quad 14$$

where

Z is the demand parameter and

θ_i is the mean

$$\theta = \left(\prod_{j=1}^{N} z_j\right)^{\frac{1}{N}} \approx z_{50\%} \quad 15$$

$$\beta = \sqrt{\frac{1}{N-1}\sum_{j=1}^{N}\left(ln\left(\frac{z_j}{\theta}\right)\right)^2} \qquad 16$$

where

z_j is the output variable for each numerical model and N is the sample number, 200 in this instance.

The fragility curves represent the probability of exceeding limit state for each seismic intensity. The seismic demand in the municipality of Palma de Mallorca is 0.04 g, corresponding to the vertical line in the fragility curve. The fragility curves, Figure 54, shows if an earthquake of 0.04 g were to happen the Mallorca Cathedral will not reach the first damage grade, since the probability is zero. At a peak ground acceleration of approximately 0.075 damage grade one is expected, at roughly 0.125 g damage grade two is predicted, and at 0.150 g collapse of the structure is anticipated.

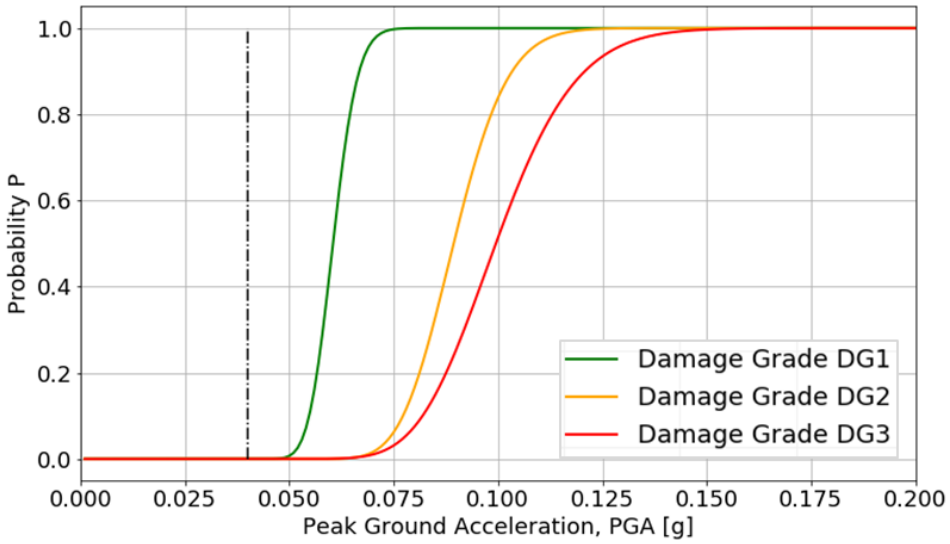

Figure 54 – Fragility Curve: Probability of Reaching Any Damage Grade for the Seismic Demand (PGA=0.04g) is Negligible

The curve of damage grade two and three are close together due to the short plateau of the bilinear curve for most the of cases

6.3 Comparison to Similar Studies

Using the developed capacity curves and fragility curves from Section 6.1, a comparison to the study by (Petromichelakis, Saloustros, & Pela, 2014), (Contrafatto, 2017) and (Bitlloch, 2018) can be completed.

In the study by Petromichelakis et al. (Petromichelakis, Saloustros, & Pela, 2014) a large difference in the collapse capacity was found. While in the elastic range of the capacity curve a smaller variance was found, which can be seen in Figure 55.

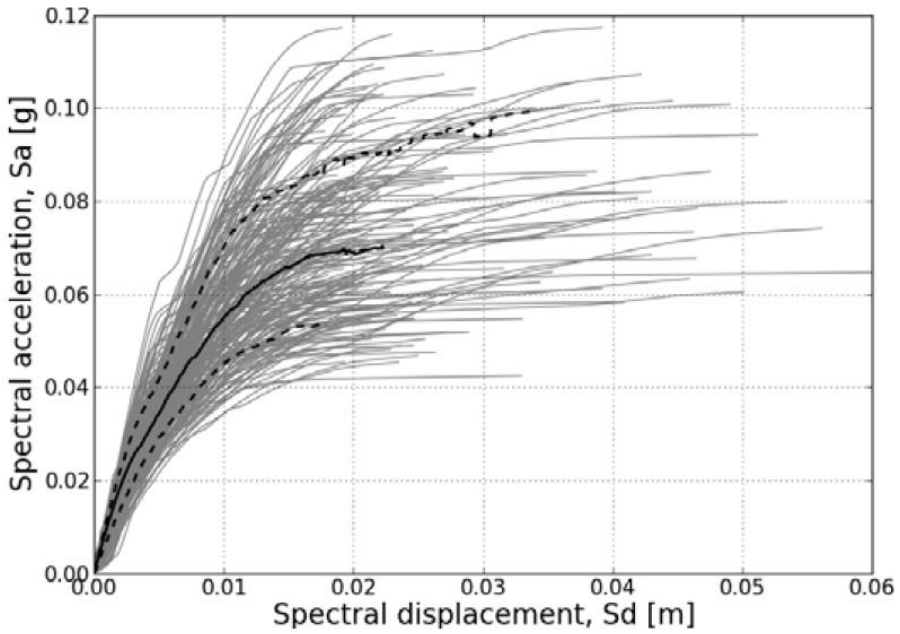

Figure 55 – Capacity Curves from Uncertainty Analysis – Royal Monastery of Santa Maria de Poblet (Petromichelakis, Saloustros, & Pela, 2014)

During the study Contrafatto developed the capacity curves for the Santa Maria Del Mar Cathedral in Barcelona, Spain, as described in Section 2.3. The capacity curves can be seen in Figure 56. Two families of curves were found.

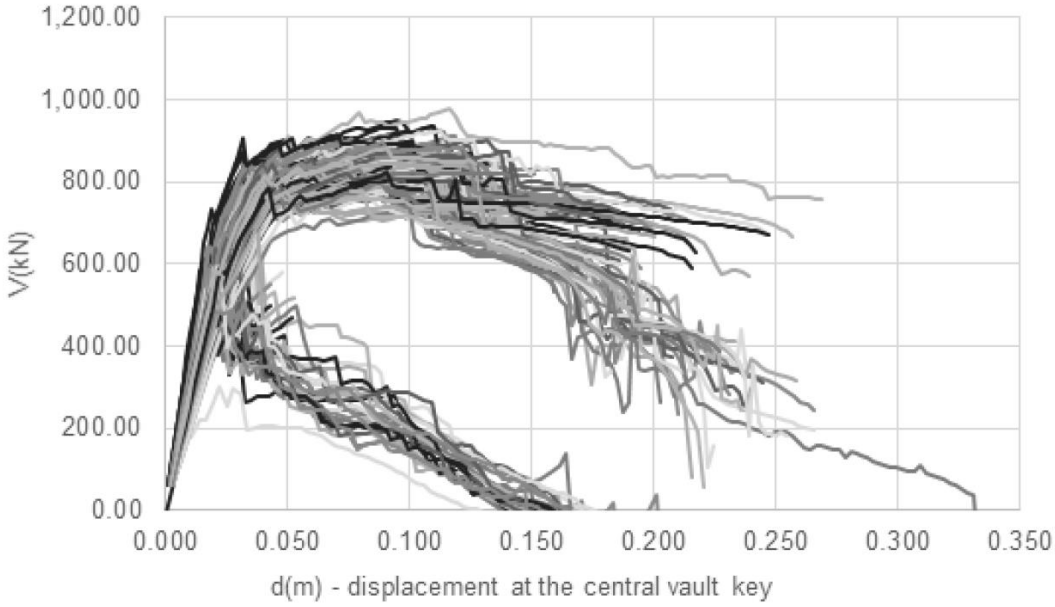

Figure 56 - Capacity Curves from Uncertainty Analysis – Santa Maria Del Mar Cathedral (Contrafatto, 2017)

In the study by Bitlloch on the Santa Maris Del Pi (Bitlloch, 2018), a large variation in the capacity curves, as seen in Figure 57. A larger variation in the plastic portion than the elastic portion of the capacity curves.

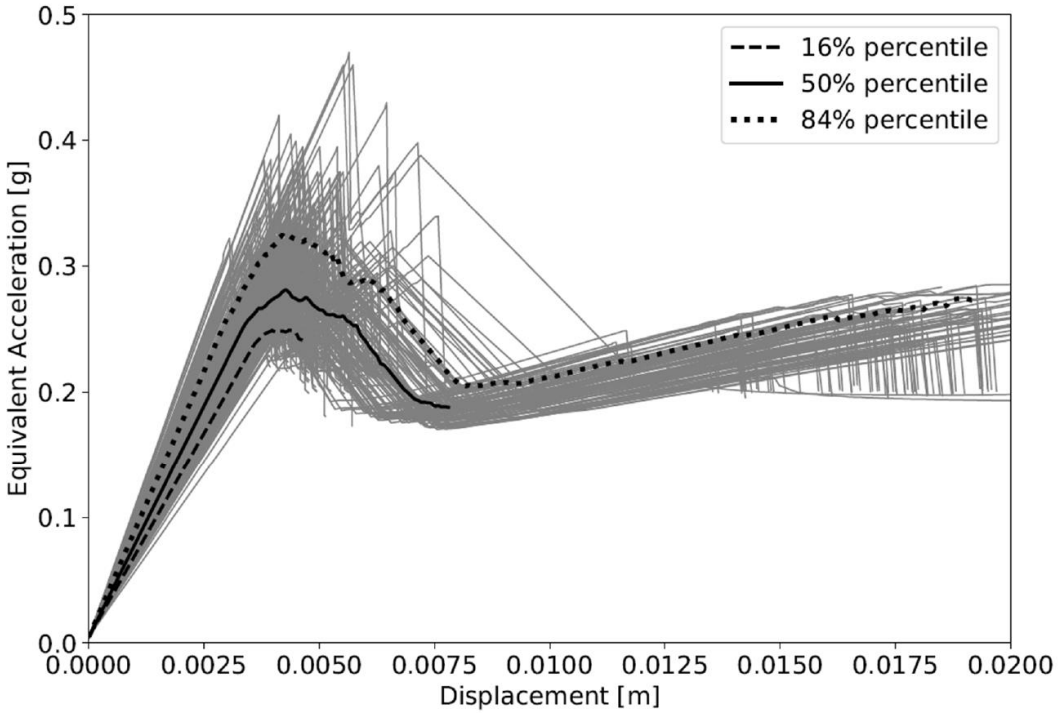

Figure 57 – Capacity Curves from Uncertainty Analysis – Santa Maria Del Pi (Bitlloch, 2018)

Similar to all of the other studies, the results found in this study the elastic portion of the capacity curves has the less difference compared to the capacity of the structure. This study the variation had less of an effect on the structural response compared to the other three structures.

7. CONCLUSIONS

7.1 Summary of Work

This research studied the vulnerability of the Mallorca Cathedral, specifically, in regard to the material mechanical property uncertainty. An equivalent two-dimensional model of a typical bay was developed and calibrated to a previous study by (Roca, Cervera, Pela, Clemente, & Chiumenti, 2013).

The effect of the uncertainty of compressive strength, tensile strength, and Young's Modulus on the seismic capacity was studied. This was done through modelling the parameters as random variables and generating a population of 200 variable values using a Monte Carlo Simulation. Each of the 200 models were assessed using nonlinear static analysis.

The probabilistic seismic assessment was completed using the guidelines of the mechanical approach as suggested by (Lagomarsino & Giovinazzi, 2006). The N2 method was applied to obtain the earthquake demand for a specific performance point. This was done by first obtaining a bilinear capacity curve, which was used to define three limit states of each model. Using these damage grades the probability of each damage grade being obtained, depending on the peak ground acceleration of an actual earthquake, was determined.

7.2 Conclusions of Research

The conclusions that can be drawn from this research are as follows.

A brittle failure of the Mallorca Cathedral during seismic loading was obtained, a local collapse of the flying arches and possible shear failure of the buttress, making the flying arches and buttresses the most vulnerable parts of the structure. The variation of mechanical properties does not significantly change the structural response. The capacity ranged from 0.0593 g to 0.08884 g, a 39.88% variation. From the obtained fragility curves, the Cathedral can be concluded to be adequate according to the seismic demand of the region of Mallorca.

The study of the Santa Maria Del Mar Cathedral (Contrafatto, 2017) was the most similar structural typology in comparison to the Mallorca Cathedral. The main differences in the results was less variation in the structural response. The Santa Maria Del Mar Cathedral had a large difference in the capacity including two families of capacity curves and three difference collapse mechanisms. While the Mallorca cathedral had significantly less variation in capacity and two similar collapse mechanisms.

7.3 Suggestions for Further Work

To further the work developed through this thesis in regard to the seismic assessment of the Mallorca Cathedral and the uncertainty in seismic vulnerability assessments the following actions are proposed.

Development of a three-dimensional model of the Mallorca Cathedral to compare the obtained results. Use of a model developed with the actual deformation to determine the effect on the capacity on the structure. Investigation into the number of analyses used for the Monte Carlo Simulation, to determine an optional number of samples. An investigation into the adequacy of the choice of the control node, top of the right column. Deeper investigation into the reasons for the lack of convergence and inability of the numerical model to capture a post-peak response. Also, similar studying using a longitudinal section of the Cathedral to obtain a more holistic assessment.

BIBLIOGRAPHY

Amellal, O., Bensaibi, M., & Grine, K. (2012). Seismic Vulnerability Index Method for Streel Structures. *World Conference on Earthquake Engineering.* Lisbon.

ATC-58. (2009). Guidelines for Seismic Performance Assessment of Buildings. Redwood City, California, USA: Applied Technology Council.

Bitlloch, C.-H. (2018, July). Vulnerability Assessment of Masonry Churches Including Uncertainty. *Masters Thesis*. Barcelona, Spain: Polytechnic University of Catalonia.

Boromeo, L. (2010). Dynamic Monitoring Analysis of Mallorca Cathedral. *Technical University of Catalonia*. Barcelona, Spain: MSc Thesis.

Bourgeois, J. (2013). *Simulation of the Effect of Auxiliary Ties Used in the Construction of Mallorca Cathedral.* Barcelona: Technical University of Catalonia.

CEB-FIP. (1993). Mode Code 1991. Thomas Telford.

Clemente, R. (2006). *Análisis estructural de edificios históricos mediante modelos localizados de fisuración.* Barcelona: Technical University of Catalonia.

CNR-DT. (2013). Guide for the Probabilistic Assessment of the Seismic Safety of Existing Buildings. Rome, Italy: Advisory Committee on Technical Recommendations for Construction.

Contrafatto, F. (2017). *Vulnerability Assessment of Monumental Masonry Structures Including Uncertainty.* Barcelona: Technical University of Catalonia.

D'Ayala, D. (2015). Assessing the Seismic Vulnerability of Masonry Buildings. *Handbook of Seismic Risk Analysis and Management of Civil Infrastructure Systems*, 334-365.

DIANA FEA. (2017). *Diana 10.2 Documentation.* Delft: DIANA FEA.

DIANA FEA. (2018). DIANA 10.2.

Eleftheriado, A. K., & Karabinis, A. I. (2013). Evaluation of Damage Probability Matrices from Observational Seismic Damage Data. *Earthquakes and Structures*.

Elyamani, A. (2015). Integrated Monitoring and Structural Analysis Strategies for the Study of Large Historical Construction. Application to Mallorca Cathedral. *Universitat Politècnica de Catalunya*. Barcelona: PhD Thesis.

Esri. (2018). *ArcGIS Spain*. Retrieved from ArcGIS: http://www.arcgis.com/home/webmap/viewer.html?webmap=7243165f096a4a409675d2c62883cd18

European Committee for Standardization. (2004). Eurocode 8: Design of structures for earthquake resistance - Part 1: General rules, seismic actions and rules for buildings. Brussels.

European Seismologic Commission. (1998). European macroseismic scale 1998 : EMS-98. Luxembourg: Centre Europèen de Géodynamique et de Séismologie.

Fajfar, P. (2000). A Nonlinear Analysis Method for Performance-Based Seismic Design. *Earthquake Spectra*, 573.

Gonzalez, J., & Roca, P. (2008). Study of Structural-Constructive Behavior of Saint Mary Cathedral in the City of Palma, Mallorca Island. Barcelona, Spain: Technical University of Catalonia.

IMIT. (2009, Feburary 2). Istruzioni per l'applicazione delle Nuove Norme Tecniche per le Costruzioni di cui al decreto ministeriale 14 gennaio 2008. Rome, Italy: Italian Ministry of Infrastructures and Transportation.

Incorporated Research Institutions for Seismology. (2011, June). *How Often Do Earthquakes Occur?* Retrieved from Incorporated Research Institutions for Seismology: https://iris.edu/hq/files/publications/brochures_onepagers/doc/EN_OnePager3.pdf

Italian Ministry of Infrastructure and Transport. (2009). Istruzioni per l'applicazione delle nuove norme tecniche per le costruzioni.

Lagomarsino, S., & Giovinazzi, S. (2006). Macroseismic and Mechanical Models for the Vulnerability and Damage Assessment of Current Buildings. *Bulletin of Earthquake Engineering*, 415-443.

Lourenco, P. B. (2009). Recent Advances in Masonry Modelling: Micromodelling and Homogenisation . *Multiscale Modelling in Solid Mechanics* , 251-294.

Magenes, G., Penna, A., Galasco, A., & Rota, M. (2010). Experimental Characterisation of Stone Masonry Mechanical Properties. *8th International Masonry Conference 2010* (pp. 247-256). Dresden: International Masonry Society.

Mark, R. (1982). *Experiments in Gothic Structure.* Cambridge: MIT Press.

Martinez, G. (2007). *Seismic Vulnerability for Middle and Long Span Masonry Historical Buildings.* Barcelona: Technical University of Catalonia.

Maynou, J. (2001). Estudi estructural del pòrtic tipus de la catedral de Mallorca mitjançan l'estàtica gràfica. *Technical University of Catalonia*. Barcelona, Spain: Graduation Thesis.

Mooney, C. Z. (1997). The Monte Carlo Principle. In C. Z. Mooney, *Monte Carlo Simulation* (pp. 3-4). Thousand Oaks: SAGE Publications.

Novelli, V. (2017, February). Hybrid Method for the Seismic Vulnerability Assessment of Historic Masonry City Centres. *PhD Thesis*. London, England: University Ccollege London.

P.I.E.T 70. (1971). Prescripciones del instituto Eduardo Torroja. Madrid: [in Spanish].

Pela, L., Bourgeois, J., Roca, P., Cervera, M., & Chiumenti, M. (2016). Analysis of the Effect of Provisional Ties on the Construction and Current Deformation of Mallorca Cathedral. *International Journal of Architectural Heritage, 10*(4), 418-437.

Perez-Gracia, V., Caselles, J., Martinez, G., & Osorio, R. (2013). Non-Destructive Analysis in Cultural Heritage Buildings: Evaulating the Mallorca Cathedral Supporting Structures. *NDT and E International*, 40-47.

Petromichelakis, Y., Saloustros, S., & Pela, L. (2014). Seismic Assessment of Historical Masonry Construction Including Uncertainty. *Proceedings of the 9th International Conference on Structural Dynamics* (pp. 297-304). Porto: EURODYN.

Roca, P., Cervera, M., Garlup, G., & Pela, L. (2010). Structural Analysis of Masonry Historical Constructions. Classical and Advanced Approaches. *Archives of Computational Methods in Engineering*, 299-325.

Roca, P., Cervera, M., Pela, L., Clemente, R., & Chiumenti, M. (2013). Continuum FE Models for the Analysis of Mallorca Cathedral. *Engineering Structures*, 653-670.

Roca, P., Clapes, J., Caselles, O., Vendrell, M., Giraldez, P., & Sanchez-Beitia, S. (2008). Contribution of Inspection Techniques to the Assessment of Historical Structures. *International RILEM Conference.* Como Lake, Italy.

Roca, P., Vacas, A., Cuzzila, R., Murcia-Delso, J., & Das, A. (2009). Response of Gothic Churches in Moderate Seismic Mediterranean Regions. *ISCARSAH Symposium on Assessment and Strengthening of Historical Stone Masonry Constructions Subjected to Seismic Action.* Mostar, Bosnia and Herzegovina: ISCARSAH.

Rubió, J. (1912). Lecture on the organic, mechanical and construction concepts of. *Anuario de la Asociación de Arquitectos de Cataluña.* Barcelona.

Salas, A. (2002). *Structural Study of the Typical Bays of Mallorca Cathedral.* Barcelona: Technical University of Catalonia.

Trip Wolf. (n.d.). *Palma Cathedral*. Retrieved from Trip Wolf: http://tripwolf.com/en/guide/show/24236/Spain/Palma-de-Mallorca/Kathedrale-La-Seu